

# Seeing with S cones

David J. Calkins

*Departments of Ophthalmology, Neurobiology and Anatomy, and Neurology and the Center for Visual Science, University of Rochester Medical Center, Rochester, NY 14642, USA*

## CONTENTS

Abstract . . . . .	255
1. Introduction . . . . .	256
2. The Distribution of S Cones in the Human Retina . . . . .	257
2.1. The density of S cones . . . . .	257
2.2. The development and structure of the S mosaic . . . . .	259
2.3. Psychophysical measures of the S mosaic . . . . .	260
3. The Distribution of S Cones in the Monkey Retina . . . . .	262
3.1. Conservation of the S opsin across most primates . . . . .	262
3.2. Comparing S cone density in primate mosaics . . . . .	262
3.3. The structure of the macaque S cone mosaic . . . . .	264
4. Linking S Acuity with a Neural Pathway . . . . .	265
4.1. S acuity and blue/yellow color vision . . . . .	265
4.2. Linking blue/yellow color vision with a neural pathway . . . . .	266
4.3. The source of the S-ON signal in primate retina . . . . .	268
4.4. Shaping the S-ON receptive field . . . . .	270
4.5. Shaping the (M + L)-OFF receptive field . . . . .	273
4.6. Setting the neutral point for the S-ON/(M + L)-OFF receptive field . . . . .	275
4.7. Conservation of the S cone and its pathways . . . . .	275
5. Signals from S Cones to Other Neural Pathways . . . . .	276
5.1. An S signal for motion . . . . .	276
5.2. Connections from S cones to other ON circuits . . . . .	278
5.3. Connections from S cones to OFF circuits . . . . .	278
6. Summary: a Lesson in Evolution . . . . .	281
6.1. A circuit for color vision . . . . .	282
6.2. The S cone and other circuits . . . . .	282
Acknowledgements . . . . .	283
References . . . . .	283

---

**Abstract**—The S cone is highly conserved across mammalian species, sampling the retinal image with less spatial frequency than other cone photoreceptors. In human and monkey retina, the S cone represents typically 5–10% of the cone mosaic and distributes in a quasi-regular fashion over most of the retina. In the fovea, the S cone mosaic recedes from a central “S-free” zone whose size depends on the optics of the eye for a particular primate species: the smaller the eye, the less extreme the blurring of short wavelengths, and the smaller the zone. In the human retina, the density of the S mosaic predicts well the spatial acuity for S-isolating targets across the retina. This acuity is likely supported by a bistratified retinal ganglion cell whose spatial density is about that of the S cone. The dendrites of this cell collect a depolarizing signal from S cones that opposes a summed signal from M and L cones. The source of this depolarizing signal is a specialized circuit that begins with expression of the L-AP4 or mGluR6 glutamate receptor at the S cone → bipolar cell synapse. The pre-synaptic circuitry of this bistratified ganglion cell is consistent with its S-ON/(M + L)-OFF physiological receptive field and with a role for the

ganglion cell in blue/yellow color discrimination. The S cone also provides synapses to other types of retinal circuit that may underlie a contribution to the cortical areas involved with motion discrimination. © 2001 Elsevier Science Ltd. All rights reserved

## 1. INTRODUCTION

Perhaps no other single neural element of the early visual pathways has mustered as much intense fascination from so diverse a scientific community as the cone photoreceptor we call “blue” or “S” for short-wavelength sensitive. In part, this fascination reflects the high degree to which the S cone and its pathways are separable *empirically* from the middle-wavelength (M) and long-wavelength (L) sensitive cones and their pathways. The S cone differs morphologically from the M and L cones in ways that the M and L cones do not differ from one another. For example, the light-funneling inner segment of the S cone is longer and wider as it joins the outer segment than is the inner segment of the M or L cone (e.g., Curcio *et al.*, 1991). Also, the glutamate-releasing axon terminal is smaller and penetrates the first synaptic layer more deeply (Ahnelt *et al.*, 1987, 1990). The synaptic features of the axon terminal distinguish the S cone at the ultra-structural level to permit study of its inner retinal pathways (Kolb *et al.*, 1997; Calkins *et al.*, 1998).

The S cone is also distinct genetically. The amino acid sequence for the S opsin is autosomal and bears little homology to the sequences for the M and L cone pigments, which are X chromosome-linked (Nathans *et al.*, 1986). Thus, the peak spectral sensitivity of the S cone is shifted from the M and L peaks by some 100 nm. This difference facilitates selective adaptation of the M and L cones and allows isolation of the psychophysical channels that serve the S cone (Stiles, 1978; Pugh and Mollon, 1979). Anatomical studies have exploited this difference in opsin structure to construct molecular markers to visualize the S cone and its mosaic across the retina (Curcio *et al.*, 1991; Bumsted and Hendrickson, 1999). These markers have demonstrated directly what psychophysicists inferred long ago, that the S cone is the “rare bird” among photoreceptors and comprises typically 5–10% of the cone mosaic depending

upon retinal location and species (see Section 3). The structure of the S mosaic is also different, forming a quasi-regular distribution outside the central retina that stands in stark contrast to the random distribution of the M and L mosaic (Curcio *et al.*, 1991). During development of the human retina, the S mosaic recedes from a central area some 0.3–0.4° in diameter (Bumsted and Hendrickson, 1999). The size of this foveal “S-free” zone differs between primate species: the smaller the eye, the smaller the zone (Martin and Grünert, 1999).

Yet, there is more to our fascination with the S cone than merely its separability. The unique morphology and spatial distribution of the S cone represent core examples in which function follows form. The taxonomy of morphological and neurochemical features that distinguish the S cone from other photoreceptors correlates with burgeoning evidence that the S cone is fundamentally different from the M and L cones in how it signals the brain. The retinal circuit for the S contribution to the color channels projects to the brain via a cluster of neurons in the thalamus that is spatially and neurochemically segregated from the far more numerous neurons dedicated to other types of cone signal (Hendry and Reid, 2000). This segregation implies a high degree of specialization in the evolution of the S pathways. Demonstrations of S input to other perceptual channels historically have been equivocal (Dobkins, 2000), and this sets the S cone apart as well. The absence of a clear anatomical link between the S cone and other non-color pathways bolsters a strong association between the S cone and a single perceptual channel and underscores the notion that seeing with S cones is *neurologically* unique.

Yet, the story may not be so simple. Converging psychophysical, physiological and anatomical evidence indicates that the S cone may not be so different from the M and L cones in how it contributes to other aspects of vision (e.g., Dougherty *et al.*, 1999; Wandell *et al.*, 1999).

The question of uniqueness becomes one of circuitry: is this contribution “second-order”, arising in the cortex from signals that piggy-back along the blue/yellow color pathway, or does it have as its roots its own neuronal line from the retina? Thus, while certain features (such as paucity) indeed distinguish the S cone and naturally limit its contribution to vision (Williams, 1986; Williams *et al.*, 1991, 1993), other features — such as its post-synaptic pathways — are more equivocal and may or may not distinguish the S cone. This review will summarize what is known about the S cone, its mosaic and the pathways involved in blue/yellow color vision and attempt to link new information about input from the S cone to other visual channels through a detailed look at its synaptic connections.

## 2. THE DISTRIBUTION OF S CONES IN THE HUMAN RETINA

The optical system of the eye, like any optical system, is subject to aberrations in focus that are wavelength-dependent. Thus, when the human eye is in focus for middle wavelengths, the point of focus for wavelengths to which the S cone is most sensitivity falls vitreal to the retina, creating a chromatic aberration of about -1 diopter (Oyster, 1999; Wandell, 1995; Williams *et al.*, 1991). As a consequence of this aberration, when the eye is accommodated under typical viewing conditions, the short end of the visual spectrum is blurred. A point of short wavelength light passing through the eye’s optics forms a retinal image in the fovea that is nearly  $0.4^\circ$  in radius at half the original intensity (Fig. 1). This attenuation means that most of the contrast that makes it through the eye’s optics and would excite S cones is contained at low spatial frequencies, less than about 5 cycles  $\text{deg}^{-1}$  (Williams *et al.*, 1993; Marimont and Wandell, 1994; see also Sekiguchi *et al.*, 1993). Indeed the eye simply does not pass significant contrast for short wavelengths at spatial frequencies greater than 7–8 cycles  $\text{deg}^{-1}$ .

Taken at face value, the eye’s optics together with what may be called “typical” viewing conditions effectively limit any evolutionary pressure to pack S cones into the photoreceptor mosaic

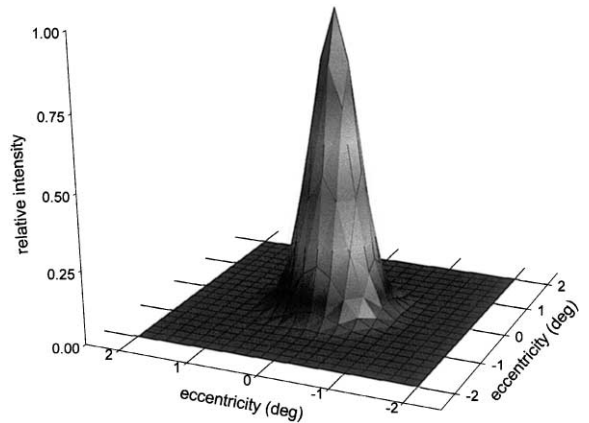


Fig. 1. Three-dimensional point spread function of the eye for short wavelength light. This was modeled as a Gaussian with half-height radius of  $0.4^\circ$ , based on the Fourier transform of a modulation transfer function with cut-off frequency of about 7 cycles  $\text{deg}^{-1}$  (Williams *et al.*, 1993). More recent measurements indicate a slightly higher cut-off frequency that would produce a more narrow point spread functions (Yoon and Williams, personal communication).

with a Nyquist rate greater than about 7–8 cycles  $\text{deg}^{-1}$ . If we approximate the S mosaic as triangular to ease the calculation, this sampling rate would correspond to an upper limit of foveal density in the human retina of 2000–2500 S cones  $\text{mm}^{-2}$ . Various anatomical measurements of the distribution of S cones in the human retina, both direct and indirect, converge to a similar estimate: S cones peak in density at about 2000 cells  $\text{mm}^{-2}$  just outside the center fovea, representing 5–10% of the cone population (see Curcio *et al.*, 1991 for review).

### 2.1. The density of S cones

Direct visualization of the S cone mosaic can be achieved by the use of sequence-specific molecular markers to distinguish S from M and L cones (Fig. 2). Measurements using antibodies generated against the S opsin yield a peak density that ranges from 1500 cells  $\text{mm}^{-2}$  at  $0.2^\circ$  eccentricity just nasal to the center fovea, to 2600 cells  $\text{mm}^{-2}$  at  $0.6^\circ$  eccentricity superior to center fovea (Fig. 3A). The average of these density measurements corresponds to about 5% of the cone population, rising to an asymptote of 8% by  $5^\circ$  eccentricity (Fig. 3B). The inner segment

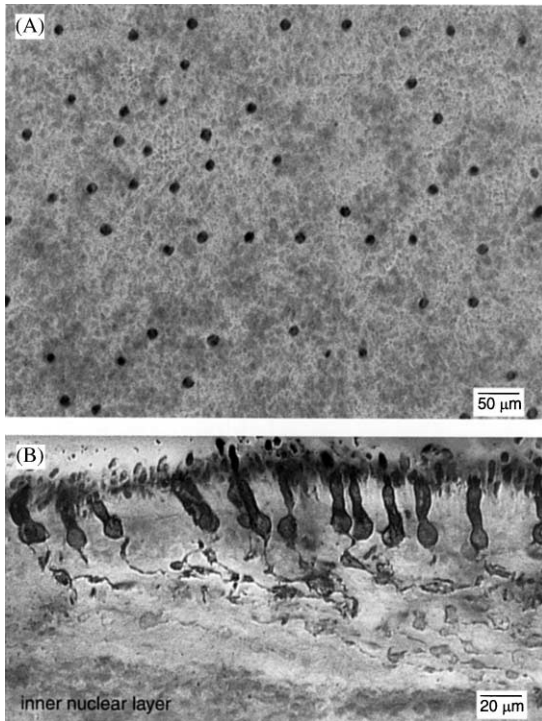


Fig. 2. The mosaic of S cones in the human retina. (A) Wholemount preparation of peripheral human retina stained using polyclonal antibodies against the S opsin (JH455, Chiu and Nathans, 1994). The S mosaic forms a quasi-regular distribution that cannot be described by a simple Poisson model. (B) Vertical section of human fovea stained using same antibodies. S cones are not absent from the fovea, as commonly thought, but reach a peak density at about  $1^\circ$  along the foveal wall. The axon terminal of each S cone is displaced with respect to the cell body via a lengthy axon or "Henle fiber". Photomicrographs from D. Calkins, unpublished.

of the S cone identified in this way is longer than that of the M or L cone and wider where it joins the outer segment (see Fig. 1 in Curcio *et al.*, 1991). Similarly, measurements using a different antibody against the S opsin or a probe for its messenger RNA yield a peak density of about  $1900 \text{ cells mm}^{-2}$  just under  $1^\circ$  eccentricity, corresponding to 8% of the cone population (Bumsted and Hendrickson, 1999). This work demonstrates another critical point: each cone that expresses the messenger RNA for the S opsin also produces the opsin. Both sets of data using molecular markers are consistent with recent densitometry measurements of cone distribution in the living human eye,

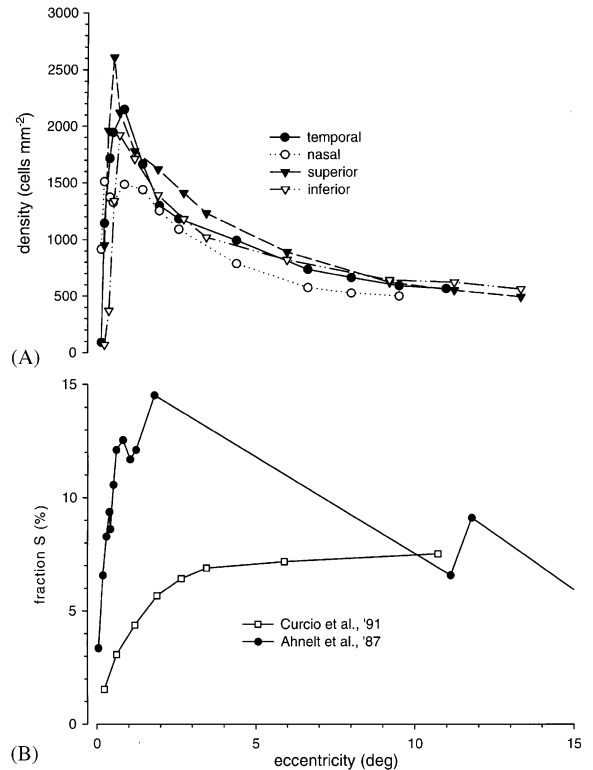


Fig. 3. The density of S cones in the human retina. (A) Measurements of the density of S cones stained using opsin-specific antibodies along the cardinal meridians. Re-plotted from Curcio *et al.* (1991). (B) The fraction of cones that are S based on immunocytochemical (Curcio *et al.*, 1991) and morphological identification (Ahnelt *et al.*, 1987).

with S cones constituting 4–5% of the foveal mosaic at  $1^\circ$  (Roorda and Williams, 1999).

The most direct way to identify an S cone is by demonstrating the expression of the S opsin, either by sequence-specific antibodies or spectral measurements. However, other molecular markers distinguish cones that in other ways are linked to the S mosaic. The validity of these markers then depend upon *post hoc* comparisons with the direct measurements. For example, antibodies raised against chicken photoreceptor membrane label about 6% of foveal cones in the human retina (Szél *et al.*, 1988). Cones labeled in this way in rabbit retina are damaged selectively with short wavelength light (Szél *et al.*, 1988), and a *post hoc* comparison demonstrates that they are identical to cones labeled with antibodies against the S opsin

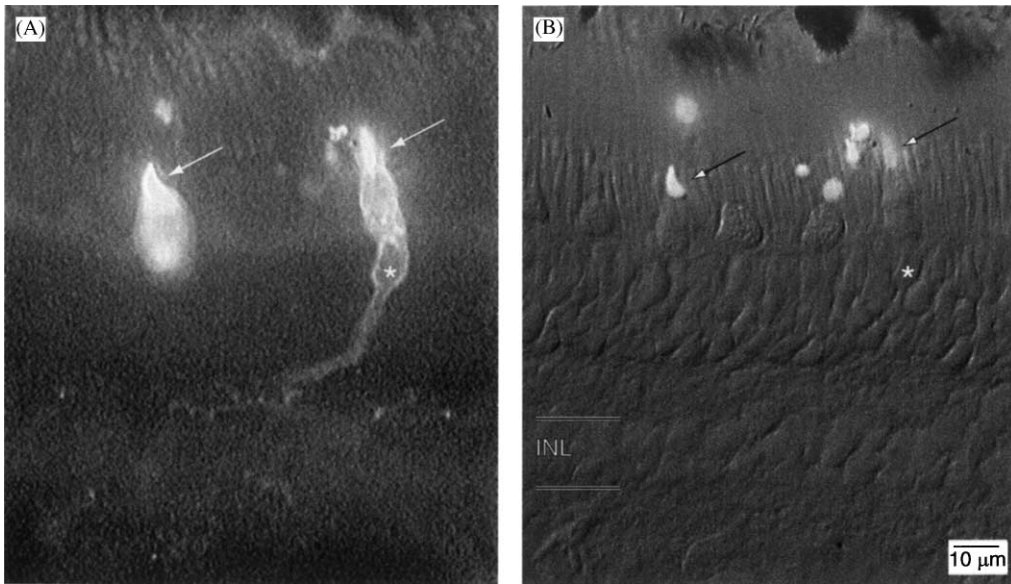


Fig. 4. Distinct antibodies both label S cones. (A) Vertical section of macaque retina stained using the JH455 antibody against the S opsin (see Fig. 2). Arrows point to the outer segment of two labeled S cones. (B) Antibodies generated against photoreceptor membranes label the same S cones (OS2, Szél *et al.*, 1988). The asterisk in both pictures marks the cell body of a labeled cone. INL: inner nuclear layer. Photomicrographs from D. Calkins, unpublished.

(Fig. 4). Similarly, cones that express low levels of the enzyme carbonic anhydrase peak at  $2000 \text{ cells mm}^{-2}$  at  $1\text{--}2^\circ$  eccentricity, where they represent 6–7% of the cone population (Nork *et al.*, 1990). These cones also bear morphological similarity to S cones identified with anti-S opsin antibodies, with inner segment longer than those of the cones expressing higher levels of carbonic anhydrase (Nork *et al.*, 1990; cf. to Curcio *et al.*, 1991). They also distribute across the retina like the S cone, constituting an average of 8% of the cones by  $3\text{--}4^\circ$  eccentricity. In contrast, inference of the S cone distribution based on morphological criteria alone (longer inner segment, smaller axon terminal) may be biased, since it yields a peak density an order of magnitude higher (Table 1, Ahnelt *et al.*, 1987).

These studies all establish firmly that S cones are not, as is often thought, absent from the fovea of the human retina (Fig. 2B). In fact, like the M and L cones, the S cone reaches peak density well within the  $1\text{--}2^\circ$  radius of the rod-free zone. What is true is that the S cone is absent in a portion of the central-most fovea or *foveola*,

where the M and L cone density peaks to about  $200,000 \text{ cones mm}^{-2}$ . Nearly every investigation summarized in Table 1 indicates a circular “S-free” zone  $0.3\text{--}0.4^\circ$  in diameter, with the highest density of S cones occurring at the boundary of this zone (Fig. 5). Indeed it would make little evolutionary sense to pack S cones into the cone mosaic where M and L cones peak. Since a point source of short wavelength light is blurred off-axis considerably (Fig. 1), S cones could contribute little to the resolution of fine spatial patterns.

## 2.2. The development and structure of the S mosaic

During neurogenesis of the primate retina, the foveal depression forms when most neurons migrate peripherally. The exception is the photoreceptor layer which migrates centrally and, in doing so, stacks the foveola with the highest possible density of outer segments; this migration continues even after birth (for review, see Curcio and Hendrickson, 1991; Hendrickson, 1998). At fetal week 15.5, S cones in the human retina

Table 1. The density of S cones in the human retina<sup>a</sup>

Method of identification	Peak density (cells mm <sup>-2</sup> )	Location	Peak (%)	Location	Ref.
Anti-S opsin	2600	0.6° (sup.)	7–8	> 5°	1
Anti-S opsin and S mRNA probe	1900	0.75	8	0.75°	2
Carbonic anhydrase activity	2000	1.5° (tem.)	6–10	> 3°	3
Inner segment and axon size	17,000	0.3° (tem.)	15	2° (tem.)	4

<sup>a</sup> Refs.: (1) Curcio *et al.* (1991); (2) Bumsted and Hendrickson (1999); (3) Nork *et al.* (1990); (4) Ahnelt *et al.* (1987). Sup: superior vertical meridian; tem: temporal horizontal meridian.

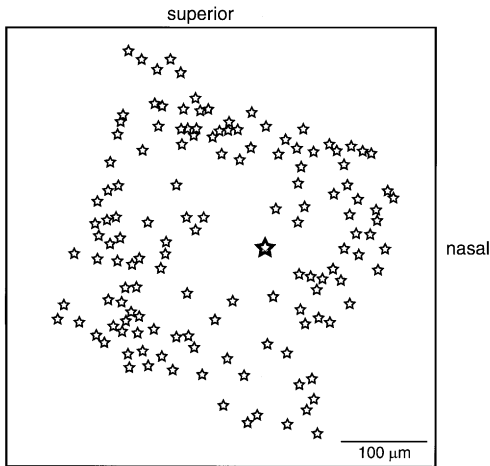


Fig. 5. The S-free zone of the human fovea. Diagram of a wholemount preparation of human foveola with S cones stained using opsin-specific antibodies (stars) flanking the region of highest density of M and L cones (large star). Re-plotted from Curcio *et al.* (1991).

distribute heavily throughout the fovea, with only a small, irregular S-free region that becomes increasingly distinct through development (Bumsted and Hendrickson, 1999). The template through which the expression of the S opsin becomes spatially regulated is not known, but it is apparently independent of the M and L mosaic (see also Curcio *et al.*, 1991). This spatial distribution depends upon retinal location. On the rim of the S-free zone, S cones pack tightly and rise to their peak density (Figs. 5 and 6A). This packing is irregular in the sense that the distance between nearest or “Voronoi” neighbors in the S mosaic is not distinguishable from the distance that would result from a random distribution; this is so throughout the fovea (Curcio *et al.*, 1991; Roorda and Williams, 1999). In this region of highest density, S cones often lie close or adjacent

to one another (Fig. 5). Small clusters of S cones are consistent with a Poisson distribution, in the same way small clusters of M or L cones arise from their simple binomial distribution (Mollon and Bowmaker, 1992; Calkins *et al.*, 1994; Roorda and Williams, 1999).

Outside of the fovea, the story is different. The further a patch of S cones lies from the point of highest S density, the less probable the distance between Voronoi neighbors in that patch arose from a random process (Curcio *et al.*, 1991). The tight clusters of S cones seen close to the foveal center also disappear as the distances between neighbors grows (see also Nork *et al.*, 1990). This is not to say the S mosaic is regular, in the sense that individual cones are placed at constant distances from one another, as in a perfect hexagonal lattice (Shapiro *et al.*, 1985), but merely that the distribution as a whole cannot be described by a simple Poisson model.

### 2.3. Psychophysical measures of the S mosaic

Before the advent of selective molecular markers, psychophysical investigations had inferred the scarcity of S cones and the structure of the S mosaic by presenting short wavelength targets to observers under conditions that selectively depress the sensitivity of M and L cones (e.g., Stiles, 1949; Williams *et al.*, 1981a, b). The foveal acuity for S-cone isolating targets varies between 5 and 15 cycles deg<sup>-1</sup>, with most measurements hovering around 10 cycles deg<sup>-1</sup> (Fig. 6B). This represents remarkable consistency given the variety of techniques between investigations. The acuity predicted by the Nyquist limit of the average peak density of the S mosaic is somewhat lower, about 6.5 cycles deg<sup>-1</sup> (Figs. 6A, B). However, the anatomical measurements depend upon averaging

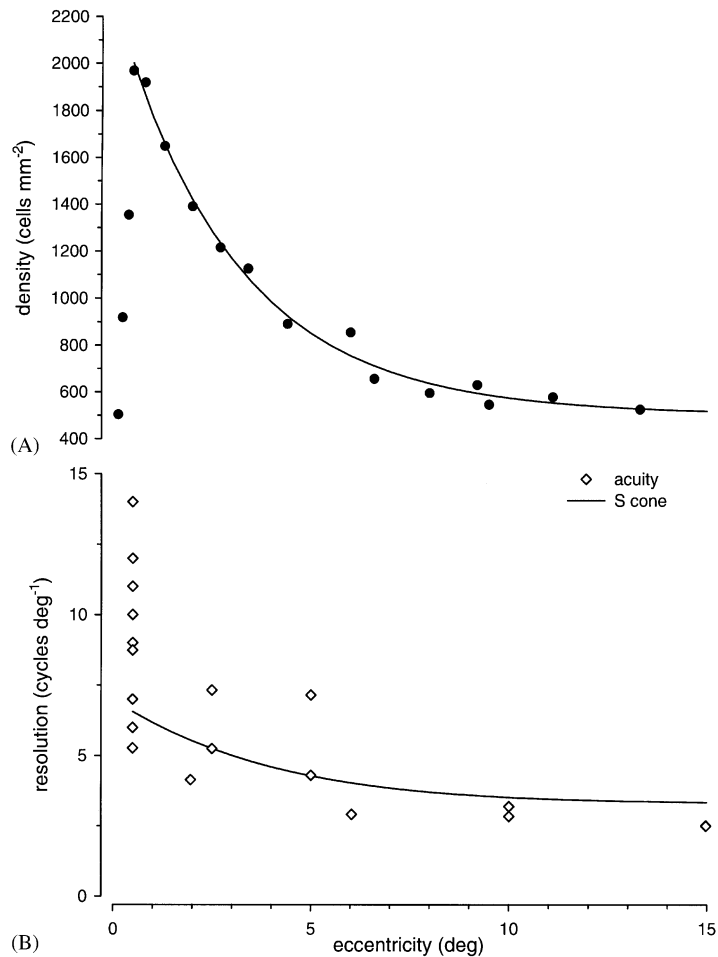


Fig. 6. The sampling frequency of S cones is comparable to S acuity in the human retina. (A) Density of S cones in human retina averaged across the cardinal meridians of Fig. 3A and fit with an exponential decay function. (B) The resolution of the S mosaic in human retina (solid curve) compared to psychophysical acuity for S-cone stimuli for normal observers and "blue cone" monochromats (symbols). Theoretical curve assumes triangular packing and is calculated as the corresponding Nyquist frequency of the average curve in (A) Psychophysical data pooled from Stiles (1949), Green (1972), Daw and Enoch (1973), Stromeyer *et al.* (1978), Mullen (1985), and Williams *et al.* (1983) for the fovea, and from Noorlander *et al.* (1983) and Hess *et al.* (1989) for the periphery.

across counting windows containing large patches of retina. The peak within any single window within the fovea can exceed 5000 cones mm<sup>-2</sup> (Curcio *et al.*, 1991), corresponding to a Nyquist limit of 10 cycles deg<sup>-1</sup>. Also, it is difficult to present psychophysically a spatially and temporally sharp stimulus to the S mosaic, and the effects of supra-Nyquist aliasing are probably substantial (Williams and Coletta, 1987; Wandell, 1995). Thus, considering these factors, there is good agreement between psychophysical peak acuity and the peak resolution of the S mosaic.

The size of the foveal S-free zone measured anatomically is 0.3–0.4° in diameter, corresponding roughly to an area of about 0.1 deg<sup>2</sup>. Psychophysicists have long recognized that the central fovea is "tritanopic": it is possible to produce a color match to a monochromatic light without a short-wavelength primary (e.g., Willmer and Wright, 1945). Indeed this classic observation is probably at the root of the misconception that the entire fovea is free of S cones. However, the careful optical measurements of Williams *et al.* (1981a, b, 1983) demonstrate that the actual tritanopic region

is only about  $20'$  in diameter, corresponding to a retinal area of  $0.09 \text{ deg}^2$  — very close to the  $0.1 \text{ deg}^2$  area measured anatomically. Outside of this zone, S cone density rises dramatically to its peak, before tapering off to an asymptote of  $500\text{--}600 \text{ cones mm}^{-2}$  beyond  $12\text{--}15^\circ$ . What psychophysical measurements there are of S-cone mediated acuity beyond the fovea agree reasonably well with the sampling rate of the S mosaic predicted by this density (Fig. 6B), perhaps slightly undershooting the S cone Nyquist by  $10\text{--}20\%$ .

Is the small difference in Fig. 6B real? Given individual differences between eyes and inevitable measurement error, there is little basis to reject the hypothesis that the spatial signal from an S cone is conserved across most of the human retina. However, that S acuity is slightly lower than the S cone Nyquist outside the fovea may imply that the representation of a single S cone in the underlying neural bottleneck becomes slightly blurred at higher eccentricities. This is certainly the case for the neurons that sample the M and L mosaic and underlie spatial acuity for luminance targets (Calkins and Sterling, 1999).

### 3. THE DISTRIBUTION OF S CONES IN THE MONKEY RETINA

The sequence of amino acids encoding the human S pigment is about as homologous with the sequences for either the M or L pigment as it is with the rod sequence (42%), indicating a common ancestral origin for these pigments. This origin is estimated at 500 million years ago (Nathans *et al.*, 1986). This is some 350 million years before the first mammals appeared during the Triassic period. Indeed the expression of a gene encoding a visual pigment with peak sensitivity in the short wavelength range of  $410\text{--}440 \text{ nm}$ , is highly (though not uniformly) conserved across mammals. Table 2 illustrates this point for familiar mammals and several species of prosimian. More thorough reviews appear elsewhere (Jacobs, 1993a,b, 1996; Tovee, 1994).

#### 3.1. Conservation of the S opsin across most primates

Most primates express the gene for the S pigment. The exceptions are nocturnal primates: the prosi-

mian bush baby *Galago garnetti* and *Galago crassicaudatus* and the New World owl monkey *Aotus trivirgatus* (Wikler and Rakic, 1990; Petry and Hárosi, 1990). The bush baby actually possesses the S gene, but does not express it (Jacobs, 1996). Among the primates that express the S gene, there is great homology between the S sequences. The human, talapoin (Old World), and marmoset (New World) sequences are  $92\text{--}96\%$  homologous, with divergence estimated between the Old and New World primates at about 43 million years ago (Hunt *et al.*, 1995). Correspondingly, the spectral sensitivity of the S cone is highly conserved across both Old and New World primate species, peaking between  $419$  and  $433 \text{ nm}$  (Table 3).

#### 3.2. Comparing S cone density in primate mosaics

The S cone is uniformly the sparsest of photoreceptors (Table 4), though its spatial distribution across the retina varies considerably between mammalian classes (Jacobs, 1993a, b; Szél *et al.*, 1994, 1996). The absolute density of the S cone in non-human primates is much higher than in the human retina (Fig. 7A). In *macaca nemestrina* and *mulatta*, the S cone density peaks at  $4000\text{--}6000 \text{ cells mm}^{-2}$  — two or three times the peak density in the human retina. In the New World marmoset *Callithrix jacchus*, the S cone density peaks at over  $10,000 \text{ cells mm}^{-2}$  — five times the human density (Martin and Grünert, 1999). The average densities in *macaca* correspond to  $5\text{--}11\%$  of all cones (Fig. 7B), while in marmoset to about  $8\%$  of the cones (Martin and Grünert, 1999). Incidentally, smaller counting fields in which variability is likely to be higher generally give much higher peak densities that give higher percentages (for *macaca*,  $7000\text{--}11000 \text{ cells mm}^{-2}$ ,  $10\text{--}26\%$ ; Bumsted and Hendrickson, 1999).

At first blush, the relatively high S density in the monkey retina would seem to support a significantly higher acuity for short wavelength targets. A density of  $10,000 \text{ S cones mm}^{-2}$  in the human retina would support resolution of about  $15 \text{ cycles deg}^{-1}$ . This is more than twice as high the resolution limit a peak density of  $2000 \text{ cones mm}^{-2}$  affords (Fig. 6). However, the high density of S cones is countered by the significantly smaller size of the macaque and marmoset eye. The foveal

Table 2. Conservation of the S opsin across mammals<sup>a</sup>

Species	Peak	Method	Investigation
Domestic dog ( <i>Canis familiaris</i> )	429	Color-matching	Neitz <i>et al.</i> (1989)
Domestic cat ( <i>Felis catus</i> )	445–455	Physiology	Weinrich and Zrenner (1983)
Tree shrew ( <i>Tupaia belangeri</i> )	410–442	MSP	Petry and Hárosi (1990)
Tree shrew ( <i>Tupaia belangeri</i> )	440	Flicker ERG	Jacobs and Neitz, (1986)
Tree shrew ( <i>Tupaia glis</i> )	440–445	MSP	Bowmaker <i>et al.</i> (1991)
Brown lemur ( <i>Eulemur fulvus</i> )	437	Flicker ERG	Jacobs and Deegan II (1993)
Ring-tailed lemur ( <i>Lemur catta</i> )	437	Flicker ERG	Jacobs and Deegan II (1993)

<sup>a</sup>MSP: microspectrophotometry; ERG: electroretinogram.

Table 3. Conservation of the S opsin across primates<sup>a</sup>

Species	Peak	Method	Investigation
Homo sapiens	419	MSP	Dartnall <i>et al.</i> (1983)
Rhesus ( <i>Macaca mulatta</i> )	430	MSP	Harosi (1987)
Cynomolgus ( <i>Macaca fascicularis</i> )	430	Suction electrode	Baylor <i>et al.</i> (1987)
Baboon ( <i>Papio papio</i> )	426–431	MSP	Bowmaker <i>et al.</i> , 1991
Marmoset ( <i>Callithrix jacchus</i> )	423	MSP	Tovee <i>et al.</i> (1992)
Squirrel monkey ( <i>Saimiri sciureus</i> )	433	MSP	Mollon <i>et al.</i> (1984)

<sup>a</sup>MSP: microspectrophotometry.

Table 4. The density of S cones in the monkey retina<sup>a</sup>

Species	Identification method	Peak density (cells mm <sup>-2</sup> )	% Range	Ref.
<i>Macaca mulatta</i>	Anti-S opsin	3000–4000	6–11	1
<i>Macaca mulatta</i>	Intraocular dye injection	5000–5500	1–8	2
<i>Macaca nemestrina</i>	Anti-S opsin	6000	5–11	3
<i>Macaca mulatta</i>	Light lesion	—	5–16	4
Baboon ( <i>Papio cynocephalus</i> )	Photo-reactive stain	6000	5–20	5
Marmoset ( <i>Callithrix jacchus</i> )	Anti-S opsin	10,000	1–8	3

<sup>a</sup>Refs.: (1) Wikler and Rakic (1990); (2) de Monasterio *et al.* (1985); (3) Martin and Grünert (1999); (4) Sperling *et al.* (1980); (5) Marc and Sperling (1977).

magnification for the macaque and marmoset retina is 223 and 128  $\mu\text{m deg}^{-1}$ , respectively, compared to 270–290  $\mu\text{m deg}^{-1}$  for the human retina (Troilo *et al.*, 1993). The corresponding Nyquist limit for the monkey therefore is only slightly higher: 8–9 cycles  $\text{deg}^{-1}$  for *macaca* and 7 cycles  $\text{deg}^{-1}$  for the marmoset, again assuming triangular packing.

There may be reason to expect a slightly higher Nyquist limit for the monkey, at least from the standpoint of evolutionary pressure. Martin and Grünert (1999) have pointed out that the spatial blurring of the retinal image for short wavelength light is less severe for the smaller macaque eye than for the human eye, and even less so for the marmoset eye. Thus, a slightly higher density of S cones, even after accounting for retinal magnifica-

tion, may correlate with a better short wavelength image. Another indication that there may be relatively less evolutionary pressure to confine the S mosaic in the monkey is the size of the foveal region lacking S cones. In the macaque retina, this region is far less well-defined than in the human retina and is no more than about half the size, 0.15–0.2° in diameter (de Monasterio *et al.*, 1985; Wikler and Rakic, 1990; Martin and Grünert, 1999). Indeed, Bumsted and Hendrickson (1999) appropriately use the term “S-sparse” zone since in their preparations of macaque fovea stained with probes against the S messenger RNA, it is difficult to measure a region in which S cones are completely absent. The eye of the of the Old World monkey *Cercopithecus aethiops* is about the same

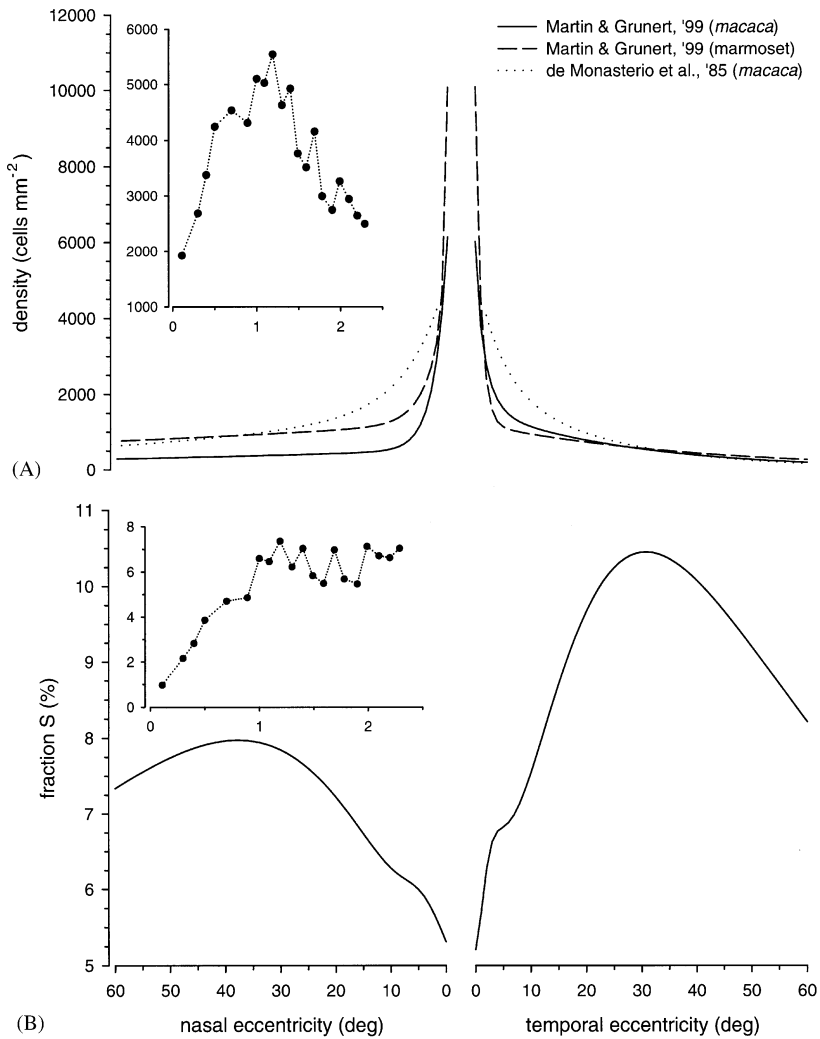


Fig. 7. The density of S cones in the monkey retina. (A) Measurements of the density of S cones along the horizontal meridian in macaque and marmoset retina. Re-plotted using exponential decay functions with parameters provided in Martin and Grünert (1999) and de Monasterio *et al.* (1985). Inset: data from macaque central retina (de Monasterio *et al.*, 1985). (B) The fraction of cones that are S in macaque retina (calculated from Martin and Grünert, 1999). Inset: fraction from macaque central retina (de Monasterio *et al.*, 1985).

size as the macaque eye and its S-free zone is comparable (Szél *et al.*, 1988). In the tiny marmoset eye, there is no S-free zone: S cones cover the entire fovea and peak in density at the center (Martin and Grünert, 1999). Martin and Grünert (1999) also point out that this is not simply a difference between Old and New World primates, because another New World monkey, *Cebus apella* has eye size similar to the macaque and a comparable S-free zone.

### 3.3. The structure of the macaque S cone mosaic

In the fetal human retina, S cones distribute freely over the entire fovea (Bumsted and Hendrickson, 1999). The S mosaic recedes completely from the central S-free zone during ensuing developmental stages. Outside this zone, the S cone density reaches its peak and the S distribution is indistinguishable from random (see above). Similarly, in the fetal macaque retina, S cones

also distribute across the entire fovea (Röhlich *et al.*, 1994; Bumsted and Hendrickson, 1999). In the mature macaque and baboon retina, S cones peak at about  $1^\circ$ , slightly more eccentric than in the human retina (Fig. 7; Marc and Sperling, 1977; Sperling *et al.*, 1980). Near this region of highest density in the macaque retina, S cones appear to distribute more regularly than in the human fovea, in that the spacing of the S cones is more nearly (though far from perfectly) triangular (de Monasterio *et al.*, 1985; Shapiro *et al.*, 1985). The S cone mosaic in the peripheral retina maintains this regularity and, in this sense, is similar to the quasi-regular distribution in the human retina (Martin and Grünert, 1999). A similar distribution exists in the baboon retina (Marc and Sperling, 1977), though not in marmoset where S cones distribute randomly throughout the retina (Martin and Grünert, 1999). Bumsted and Hendrickson (1999) provide an insightful discussion of the developmental mechanisms underlying the S distribution and its relationship with the M and L cone mosaics.

#### 4. LINKING S ACUITY WITH A NEURAL PATHWAY

There is fairly good agreement between spatial acuity for S-cone isolating stimuli and the sampling limit of the S mosaic based on density measurements (Fig. 6B). For a given psychophysical task, spatial resolution is limited by the neural bottleneck determining detection for that task, and it is reasonable to associate this bottleneck with a particular type of retinal ganglion cell (Wässle and Boycott, 1991). One might expect then a particular type of ganglion cell to not only sample the photoreceptor mosaic with close to the frequency of the S cone, but also to collect S signals such that the integrity of the signal from each S cone is represented in the mosaic of that ganglion cell. In this way, the neural image of the S mosaic could be preserved with minimum loss of resolution. The question becomes one of linking one or more psychophysical channels with a particular retinal circuit serving a particular type of ganglion cell (see also Dacey, 1999).

#### 4.1. S acuity and blue/yellow color vision

Visual scientists have long associated seeing with S cones with an “opponent” psychophysical channel that subserves the discrimination of blue from yellow hues. Experiments in which observers adjust blue and yellow lights in mixture until neither hue is perceived and direct measurements of wavelength sensitivity indicate a spectral signature for the blue/yellow channel described by S-(M+L), or (M+L)-S, depending on how the data are represented (for review, see Lennie and D’Zmura, 1988; Rodieck, 1998). In this expression, the relative weight of each cone type depends upon the cone’s inherent sensitivity and upon the adaptive conditions; these factors scale that cone’s input to the channel. Typically, the S-(M+L) subtractive combination produces a short wavelength peak where the S signal dominates, a middle wavelength peak where the M+L signal dominates, and a sharp decline or “neutral point” in sensitivity where the two terms are similar, around 500 nm. Where the S signal is greater, the channel signals “blue”; where the M+L signal is greater, the channel signals “yellow”. When the two signals are appropriately balanced, say with a 500 nm light, the perceived hue is neither blue nor yellow and is said to be in “blue/yellow equilibrium” (Hurvich and Jameson, 1957; Larimer *et al.*, 1975; Pugh and Larimer, 1980). This combination of cone inputs represents the minimal condition for the channel and does not preclude interactions with other channels to produce mixed color percepts, such as violet. Critically, the S and M+L components of the blue/yellow channel are spatially *co-extensive*, so that at the resolution limit of the channel, an alternating spatial pattern of blue and yellow lights will appear as a single, neutral percept.

It is somewhat presumptive to equate the acuity measured for an S-cone isolating stimulus (Fig. 6B) with the spatial resolution of the blue/yellow channel. This is an idea most are willing to accept, especially in the absence of hard evidence that S cones feed into additional neural pathways not associated with color opponency (but see below). There is no *a priori* reason why a particular acuity task ought to tap a color channel. Determination of whether this is so depends upon

other factors, such as perceptual attributes associated with the stimulus, like its color appearance. A definitive test would be to determine whether threshold additivity, which holds for luminance grating acuity (e.g., Myers *et al.*, 1973), is in fact violated for alternating blue and yellow gratings. Nevertheless, despite these ambiguities, it is useful to compare S acuity with the neuronal mosaics likely to contribute to blue/yellow opponency.

#### 4.2. Linking blue/yellow color vision with a neural pathway

Psychophysical measures of the blue/yellow channel link its physiological basis to a neural pathway in which signals from S cones converge *antagonistically* with those from M and L cones (reviewed in Lennie and D'Zmura, 1988). This pathway is denoted "S/(M+L)", where "/" indicates spatially co-extensive antagonism between S cones and the sum of M and L signals. This antagonism is established early in the visual pathways. A population of relay neurons in the lateral geniculate nucleus (Wiesel and Hubel, 1966; Dreher *et al.*, 1976; Marroco and De Valois, 1977; Derrington and Lennie, 1984) and ganglion cells in the retina (de Monasterio and Gouras, 1975; de Monasterio, 1978; Zrenner, 1983a,b; Dacey, 1996) demonstrate the appropriate spectral signature (neutral point at 500 nm) and also the appropriate spatial profile, in which the S and M+L components are co-extensive (Fig. 8; for review, see Rodieck, 1991). Most of the so-called "blue/yellow" cells in these recordings responded with excitation at the onset of S stimulation and at the offset of M+L stimulation, i.e., S-ON/(M+L)-OFF; a small number had the reverse configuration (discussed below).

It is difficult to glean from the early extracellular recordings how often either the S-ON/(M+L)-OFF geniculate cell or its ganglion cell counterpart sample the photoreceptor mosaic. A critical step forward was to match the morphology of a ganglion cell with the S-ON/(M+L)-OFF physiological receptive field. Intracellular recording of spectral responses from macaque ganglion cells with subsequent staining of their dendritic trees revealed a "small bistratified" ganglion cell, with one dendritic arbor deep in the ON stratum of the inner retina and another dendritic arbor, co-

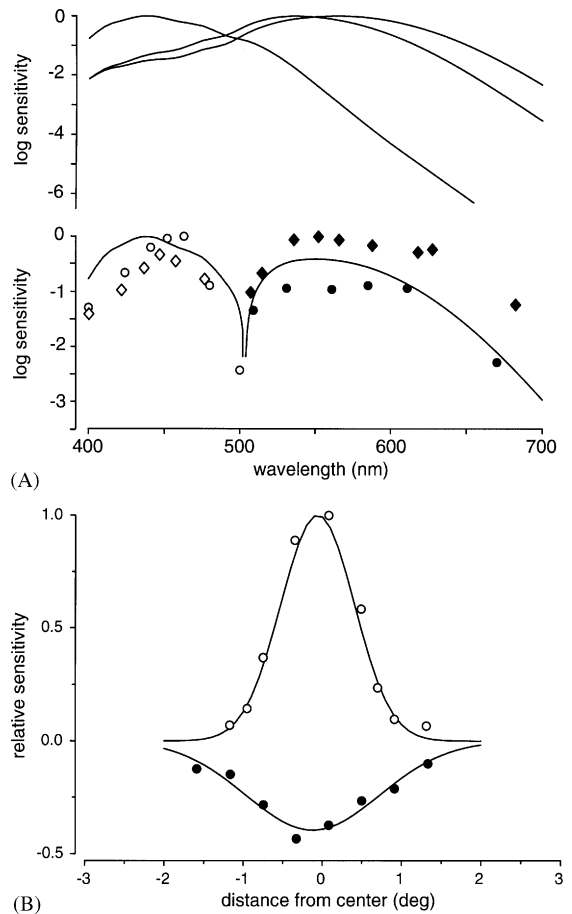


Fig. 8. The spectral and spatial profiles of the S-ON/(M+L)-OFF receptive field. (A) Upper graph: spectral sensitivity of S, M, and L cones (from Baylor *et al.*, 1987) corrected for absorption by optical media (Wysocki and Stiles, 1983); S cone spectral sensitivity extrapolated by linear regression for wavelengths greater than 600 nm. Lower graph: two sets of spectral sensitivity measurements from S-ON/(M+L)-OFF ganglion cells (re-plotted from Zrenner, 1983a,b). Open symbols represent excitation to light onset, filled symbols represent excitation to light offset. The computed spectral sensitivity (solid curve), calculated as the absolute difference between S and (M+L), assumes that M and L cones are present in equal numbers and scales the S and M+L signals according to their synaptic weights for a foveal ganglion cell (re-plotted from Calkins *et al.*, 1998). (B) Spatially co-extensive S-ON (open symbols) and (M+L)-OFF (filled symbols) responses of a small bistratified ganglion cell. Data re-plotted from Dacey (1996) and fit to a simple Gaussian (solid curves).

spatial with but slightly smaller than the first, in the OFF stratum (Dacey and Lee, 1994). The cell responds with excitation to the onset of short

wavelength light and to the offset of middle and long wavelengths, suggesting that the bistratified morphology correlates with segregated ON and OFF inputs.

The mosaic of this same small bistratified ganglion cell had already been mapped by micro-injection in the human and macaque retina for the parafovea and beyond (Dacey, 1993). These injections provide precise measurement of the cell's dendritic arbor as a function of eccentricity (Fig. 9). Assuming adjacent arbors "tile" the retina, the average diameter of the dendritic tree provides an estimate of the cell's density and therefore its Nyquist sampling rate (Dacey, 1993).

Fig. 10 illustrates a key point for the human retina. Individual differences between retinas are likely to be substantial, and the great variability between the size of dendritic arbors at a particular eccentricity (e.g., Fig. 9) confounds the estimate of density. Nevertheless, the estimated sampling rate of the small bistratified cell agrees reasonably well with measurements of S acuity. The Nyquist rate for the fovea is based on identification of the ganglion cell in *macaca* using electron microscopy (Calkins *et al.*, 1998). The finding there was one small bistratified cell for every S cone, and there is little reason to doubt that the same holds for the human fovea. Thus, the small bistratified ganglion

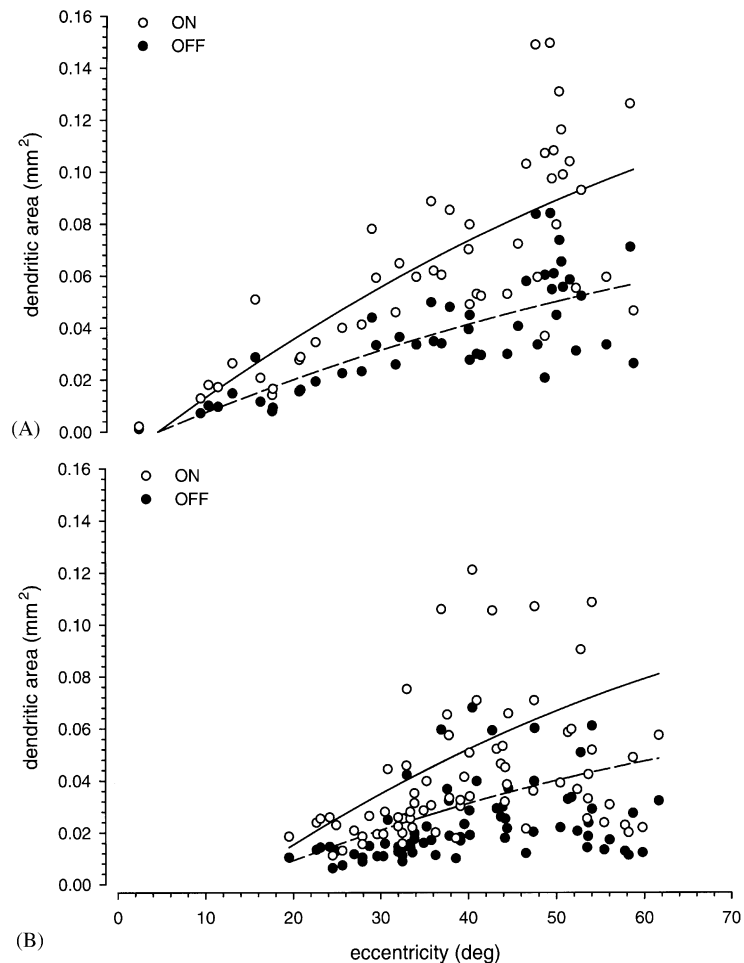


Fig. 9. The area of the dendritic tree of the small bistratified ganglion cell. (A) Area of dendritic tree in ON (open symbols) and OFF (closed symbols) regions of the inner plexiform layer of human retina. OFF area is scaled from ON area assuming OFF tree is 75% the diameter of the ON tree. Solid curves are best-fitting polynomials. (B) Same as A for macaque retina. Data for ON tree re-plotted from Dacey (1993).

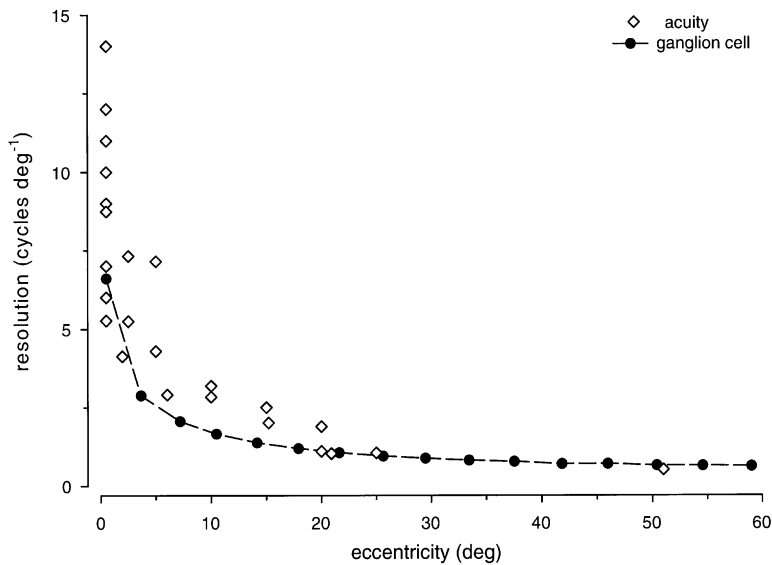


Fig. 10. The sampling frequency of the small bistratified ganglion cell matches S acuity in the human retina. The sampling frequency for the ganglion cell is calculated as the corresponding Nyquist frequency assuming triangular packing and based on the density measurements of Dacey (1993) outside of the fovea and of Calkins *et al.* (1998) for the fovea. Acuity measurements same as in Fig. 6B.

cell is likely dense enough to support the spatial acuity of the blue/yellow channel across eccentricity.

#### 4.3. The source of the S-ON signal in primate retina

A retinal circuit optimized to carry color information should subtract the signals of one cone type from those of other types to reduce the redundancy resulting from overlapping spectral sensitivities (Buchsbbaum and Gottschalk, 1983; Derrico and Buchsbbaum, 1991). To optimally fill the dynamic range of the ganglion cell with a pure spectral-difference signal, its receptive field ought to be spectrally but not spatially antagonistic (Calkins and Sterling, 1999). The small bistratified ganglion cell with its S-ON/(M+L)-OFF receptive field apparently achieves this (Fig. 8; Dacey, 1996).

What is the source of the pure S signal for the ganglion cell? In the ON stratum, the ganglion cell dendrites ramify at the border between the ganglion cell and the inner synaptic layer. There, the dendrites intermingle with the axon terminals of the so-called “blue cone” or “S” bipolar cell. This is the only bipolar cell in the mammalian retina whose dendrites pass beneath cone terminals without contact to collect synapses only from a

few widely spaced S cones (Fig. 11A; Mariani, 1984; Kouyama and Marshak, 1992; Wässle *et al.*, 1994; but see Kolb *et al.*, 1992). In the fovea, each S bipolar cell forms about 40 pre-synaptic active zones (or “ribbons”; Figs. 11B and C). Most of these are directed to a small number of small bistratified ganglion cells, and each ganglion cell in turn is post-synaptic to 2–3 S bipolar cells (Fig. 11D; Calkins *et al.*, 1998). Amacrine cells also provide synapses to both the bipolar cell terminal and the ganglion cell dendrites (Dacey, 1993; Calkins *et al.*, 1998). These synapses are likely inhibitory (glycinergic or GABAergic), so the only source of excitatory S input to the ganglion cell is via the S bipolar cell.

Excitation in the retina is conveyed through the release of glutamate, both at the cone → bipolar cell synapse and the bipolar cell → ganglion cell synapse (Massey, 1990). Other types of ganglion cell are known to express *ionotropic* glutamate receptors, which open cation channels upon binding glutamate (Cohen and Miller, 1994; Zhou *et al.*, 1994; Peng *et al.*, 1995; Qin and Pourcho, 1995; Lukasiewicz *et al.*, 1997). Thus, the S bipolar cell with light stimulation is likely to release glutamate that opens cation channels on the dendrites of the S-ON/(M+L)-OFF ganglion cell.

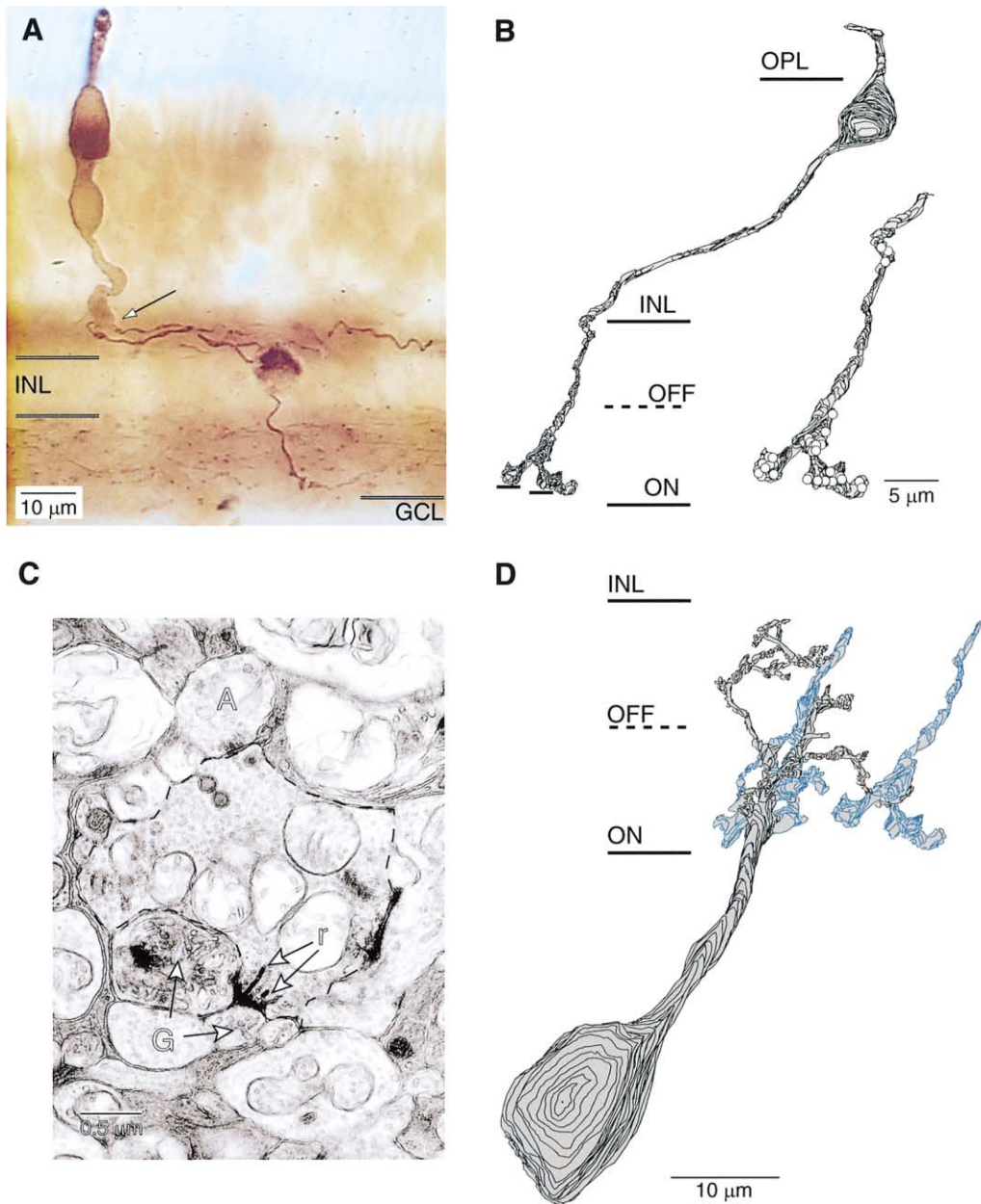


Fig. 11. Circuitry for S-ON response in small bistratified ganglion cell. (A) Dendrites of an S bipolar cell in macaque retina, stained using antibodies against cholecystokinin (CCK, see Kouyama and Marshak, 1992), collect from the axon terminal (arrow) of an S cone stained using JH455 (see Fig. 2A). INL: inner nuclear layer; GCL: ganglion cell layer. Photomicrograph from D. Calkins, unpublished. (B) Reconstruction of an S bipolar cell in macaque fovea. Axon courses through the OFF region of the inner plexiform layer before bifurcating deep in the ON region to form over 30 pre-synaptic active zones (circles). The axon also forms some active zones at the border between the OFF region and the inner nuclear layer (INL). (C) Axon terminal of S bipolar cell outlined with dark line (high magnification electron micrograph). Ribbon synapses (r) are pre-synaptic at a "dyad" of two ganglion cell dendrites (G). Amacrine cell process (A) is pre-synaptic to the bipolar cell terminal at a conventional synapse (dark clustering of vesicles). (D) Reconstruction from electron micrographs of a small bistratified ganglion cell in macaque fovea and the axon terminals of the two S bipolar cells (blue traces) that provide its ON response to short wavelengths. (B–D) modified from Calkins *et al.* (1998).

Because increased light *decreases* the rate of glutamate release from photoreceptors, an ON bipolar cell must express a *metabotropic* glutamate receptor that uses a second-messenger cascade to invert the sign of polarization at the cone synapse (Vardi *et al.*, 1993; Shiells and Falk, 1995). ON bipolar cells in the mammalian retina probably all express the L-AP4 or mGluR6 receptor at their dendrites (Nakajima *et al.*, 1993; Euler *et al.*, 1996; Hartveit, 1997; Vardi *et al.*, 1998). Indeed the S bipolar cell apparently does so as well (Vardi *et al.*, 2000; Fig. 12), implying that the small bistratified cell's ON response to S stimulation arises through excitation mediated by mGluR6 at the first synapse in the circuit.

#### 4.4. Shaping the S-ON receptive field

The mosaic of S bipolar cells is visualized using antibodies that recognize glycine-extended forms of precursors for cholecystokinin (CCK). This mosaic is tightly correlated with the mosaic of S cones (Fig. 13B), each forming a non-random distribution (Kouyama and Marshak, 1997). The S

cone and some types of cone bipolar cell share certain transcription events during development (Chiu and Nathans, 1994; Chen *et al.*, 1994). Among these cells may be the S bipolar cell, in which case a ready-made mechanism for spatial dependence may be built into the genome. Where S cones peak in density, there is about one S bipolar cell for each S cone. This ratio soon rises to an average of about two, where it is maintained over most of the retina (Fig. 13C). Direct visualization of contacts between S cones and S bipolar cells show each cone diverges typically to two bipolar cells, though some S cones contact up to 5 (Kouyama and Marshak, 1992; Wässle *et al.*, 1994; Calkins *et al.*, 1998). These contacts invariably occur where dendrites of the S bipolar cell penetrate the narrow invaginations of the S-cone terminal that mark active zones of glutamate release (see Section 5.2). Table 5 lists for each of five S bipolar cells post-synaptic to a particular foveal S cone the number of invaginating dendrites contributed (see Calkins, 2000). In turn, each S bipolar cell collects from 1–3 S cones, depending upon the number of S cones in proximity to the

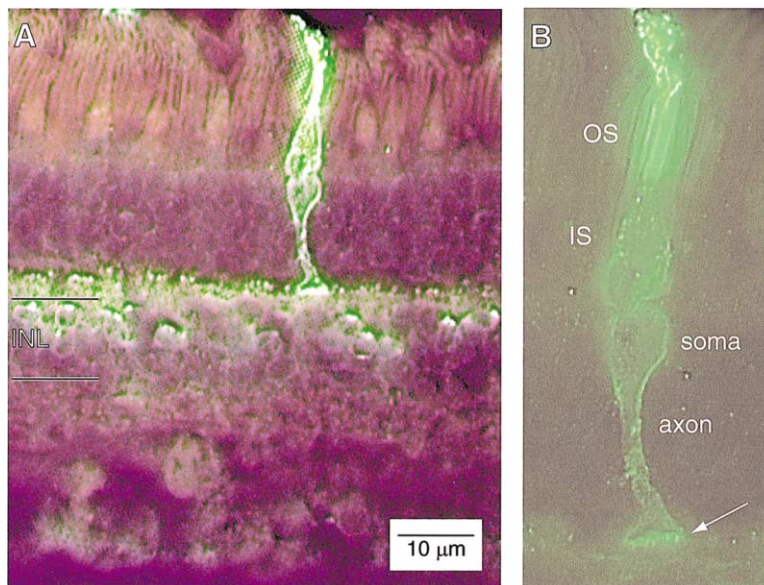


Fig. 12. A metabotropic glutamate receptor mediates depolarizing signals from S cones. (A) Vertical section of macaque retina stained using the JH455 antibody against the S opsin and a polyclonal antibody against the L-AP4 sensitive metabotropic glutamate receptor, mGluR6 (Vardi *et al.*, 1998; 2000). The mGluR6 receptor localizes to discrete puncta on the dendrites of ON bipolar cells at the base of the photoreceptor axon terminal (see Vardi *et al.*, 2000). (B) Higher magnification view of the S cone with mGluR6 clustered beneath the axon terminal where the dendrites of the S bipolar cell penetrate. Photomicrograph from D. Calkins, unpublished.

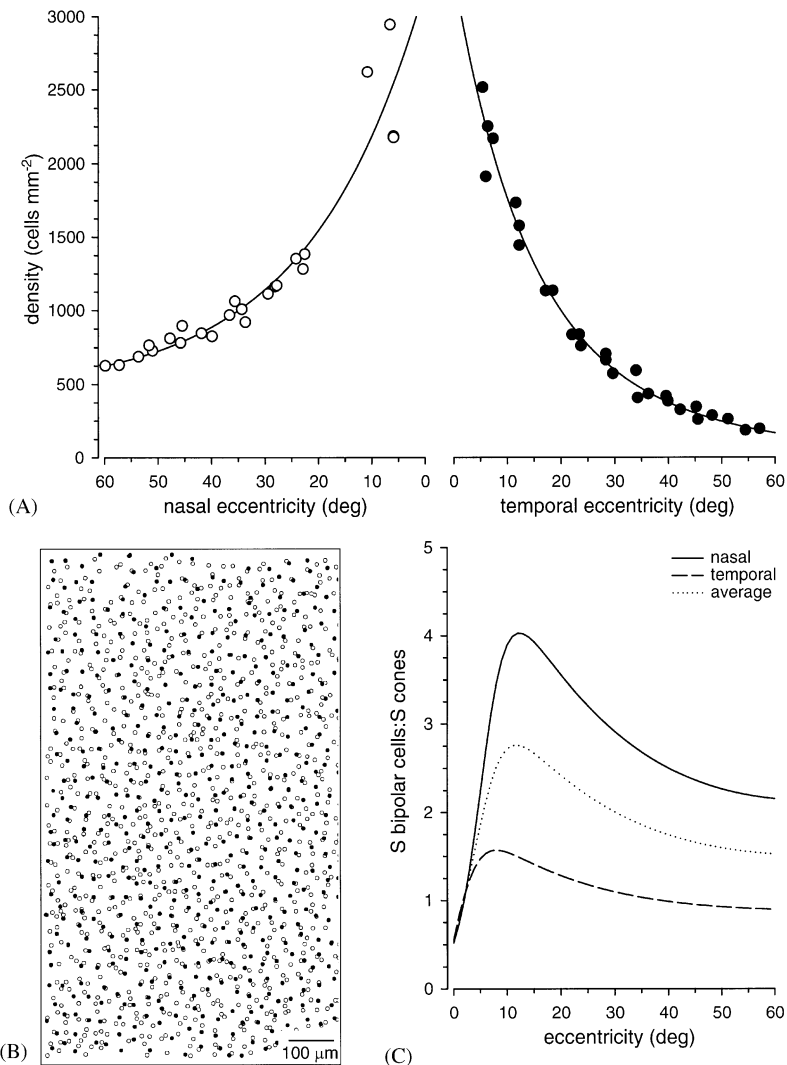


Fig. 13. The mosaic of S bipolar cells in macaque retina. (A) Density of S bipolar cells stained using antibodies against CCK along horizontal meridians of macaque retina. Re-plotted from Kouyama and Marshak (1992) and fit with exponential decay functions. (B) The mosaics of S bipolar cells (open symbols) and S cones (filled symbols) are tightly correlated and form non-random distributions in macaque retina (modified from Kouyama and Marshak, 1997). (C) The ratio of S bipolar cells to S cones in macaque retina calculated from the decay functions in A and in Fig. 7 for the data of Martin and Grünert (1999). Over most of the retina, the signal from the mosaic of S cones is “up-sampled” within the denser mosaic of S bipolar cells.

Table 5. Divergence at an S cone<sup>a</sup>

S Bipolar cell	Invaginating dendrites
1	16
2	13
3	2
4	1
5	1

<sup>a</sup> Modified from Calkins (2000).

dendritic tree (Kouyama and Marshak, 1992; Wässle *et al.*, 1994). Thus, there is both divergence and convergence at the level of the cone → bipolar cell synapse.

Reconstructions of the small bistratified cell with electron microscopy indicate that in the macaque fovea, the ganglion cell collects from about three S cones via 30–35 synapses from 2–3 S bipolar cells (Fig. 14A; Calkins *et al.*, 1998).

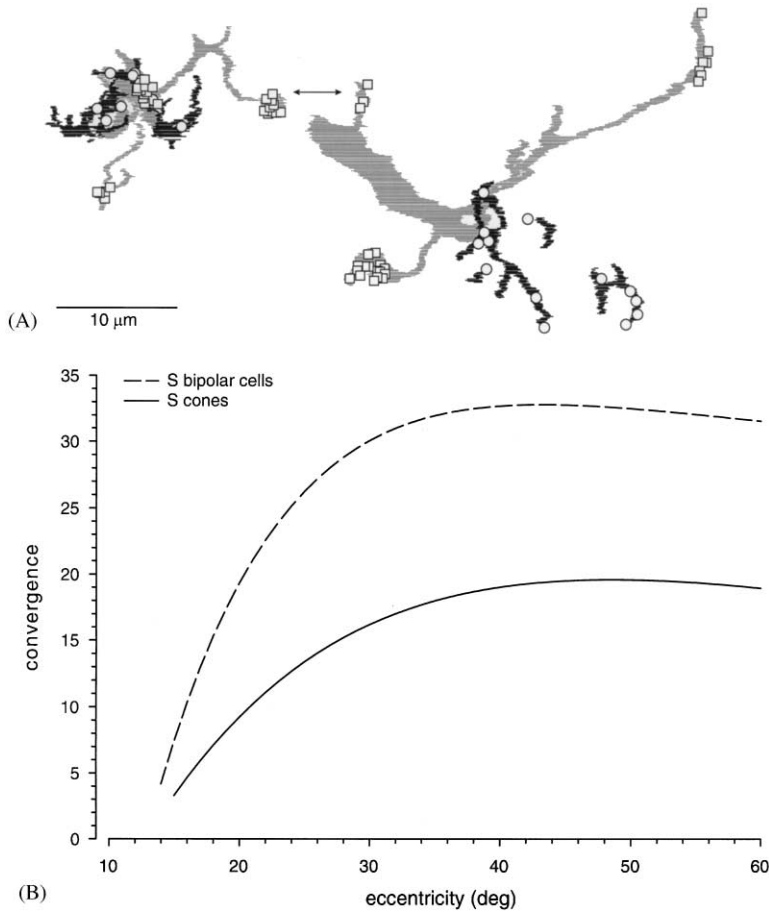


Fig. 14. Convergence of S cone circuitry to the small bistratified ganglion cell. (A) Tangential view of the dendritic arbors of two adjacent small bistratified ganglion cells and their synapses. Dendrites in the ON stratum of the inner plexiform layer (light shading) receive, respectively, 34 and 32 contacts from S bipolar cells, while dendrites in the OFF stratum (dark shading) receive, respectively, 15 and 13 contacts from diffuse bipolar cells. Some contacts are hidden by others. Arrow marks synapses from an S bipolar cell that contacts both ganglion cells. Modified from Calkins *et al.* (1998). (B) Convergence of S cones and S bipolar cells to the small bistratified cell in macaque retina. Over most of the retina, nearly twice as many S bipolar cells as S cones converge on the ganglion cell. Convergence calculated as the product of dendritic tree area in ON stratum (fitted polynomial in Fig. 9B) and S cone or S bipolar cell density (Figs. 7 and 13).

Outside of the fovea, the dendritic tree of the ganglion cell in the ON stratum encompasses increasing expanses of retina as the cell's density declines (Figs. 9 and 10). Consequently, the convergence of both S cones and S bipolar cells increases (Fig. 14B). A small bistratified cell at 10–20° eccentricity collects from 5 to 10 S cones, while cells at 25° eccentricity and further collect from 10 to 20 S cones. These numbers are consistent with recent multi-electrode recordings from S-ON/(M+L)-OFF cells which indicate convergence of

5–15 S cones between 20 and 50° eccentricity (Chichilnisky and Baylor, 1999).

These multi-electrode recordings actually illustrate several key points. The signals from individual S cones to the receptive field of the ganglion cell sum linearly: their combined contribution predicts the net response of the cell to S stimulation. Also, the relative strength of these signals varies between cones, with one S cone providing the dominant input. Conversely, while a particular S cone may contribute to the receptive fields of

neighboring ganglion cells, that S cone provides the dominant input to only one ganglion cell (Chichilnisky and Baylor, 1999).

These results are consistent with predictions based on circuitry. While multiple S cones may contact a particular S bipolar cell, one of these provides 70% or more of the synaptic input. Similarly, at the next synaptic level, a single S bipolar cell dominates in providing synapses to a small bistratified ganglion cell. The result of these two levels of synaptic weighting is that a single S cone provides the dominant signal to a particular ganglion cell (Calkins *et al.*, 1998; Chichilnisky and Baylor, 1999; Calkins, 2000). Each S cone diverges typically to two S bipolar cells (Kouyama and Marshak, 1992; Wässle *et al.*, 1994), which in turn diverge each to about 2 small bistratified cells (Calkins *et al.*, 1998). With twice as many S bipolar cells as S cones (Figs. 13B and C), the ganglion cell can receive multiple, parallel copies of the signal from a particular S cone, thus bolstering the integrity of that cone's representation in the receptive field. Furthermore, with so many S bipolar cells, the potential for overlapping S-ON/(M+L)-OFF receptive fields is immense. Thus, it is not surprising that one S cone can contribute to several ganglion cells, while providing dominant input to only one (Chichilnisky and Baylor, 1999). In this way, the circuitry of the small bistratified cell may counter-balance the sparseness of the S mosaic and contribute to the perceptual contiguity of S-isolating stimuli (Brainard and Williams, 1993).

If every S cone is so represented, the density of the small bistratified cell ought to match the S cone density. This is clearly so in the primate fovea (Calkins *et al.*, 1998). Outside of the fovea, in human retina, the disparity between the sampling of the small bistratified cell and the sampling of the S mosaic is small (cf. Figs. 6 and 10), too small to reject the hypothesis given methodological differences and inter-retina variation. The density of the ganglion cell for extra-foveal retina in *macaca*, however, falls dramatically short of the S cone density (Dacey, 1993). For example, in the periphery, the ganglion cell density asymptotes to about 30 cells mm<sup>-2</sup> (Fig. 13 in Dacey, 1993), while the S cone density is still higher by a factor of 4–5 (Fig. 7). This may seem to contradict the

physiological result in monkey retina showing each S cone as the dominant input to its own ganglion cell (Chichilnisky and Baylor, 1999). However, the estimate of ganglion cell density is based on dendritic field size and inter-cell spacing, both of which are subject to considerable variability and probably lead to an underestimation of the actual density.

#### 4.5. Shaping the (M+L)-OFF receptive field

The small bistratified cell fires with the offset of yellow light, and this OFF response originates in M and L cones (Dacey and Lee, 1994; Chichilnisky and Baylor, 1999). What inter-neurons carry the (M+L)-OFF signal? In the OFF stratum of the inner plexiform layer, the ganglion cell collects synapses from the DB2 and DB3 types of “diffuse” bipolar cell (Figs. 14A and 15A; Calkins *et al.*, 1998). These bipolar cells are so named because their dendritic trees collect from each cone they span (Boycott and Wässle, 1999). There, at the cone terminal base, the dendrites of the DB2 and DB3 cells likely express ionotropic glutamate receptors (Morigiwa and Vardi, 1999), which would *open* cation channels upon binding glutamate with the offset of M and L stimulation. Furthermore, both of these diffuse cells provide synapses to the parasol OFF ganglion cell (Calkins, 1999), which is known to also fire at the offset of M and L cone stimuli (Dacey and Lee, 1994; Dacey, 1996). Thus, through distinct bipolar cell circuits, S cones and M and L cones effect opposing currents in the ganglion cells, and their joint stimulation produces concurrent S-ON and (M+L)-OFF responses.

In the macaque fovea, the axon terminals of the S cone bipolar cell provide 30–35 synapses to the ganglion cell in the ON stratum (Calkins *et al.*, 1998). In the OFF stratum, the axon terminals of the DB2 and DB3 cells provide only about half as many synapses (Fig. 14A). Consequently, about 70% of the excitation in the receptive field is carried via the S-cone circuit. This difference in synaptic weight, when convolved with the number of converging cones (Fig. 15B), can account for the 40% difference in amplitude between the S-ON and (M+L)-OFF components of the receptive field (compare Figs. 8B and 15C). The difference

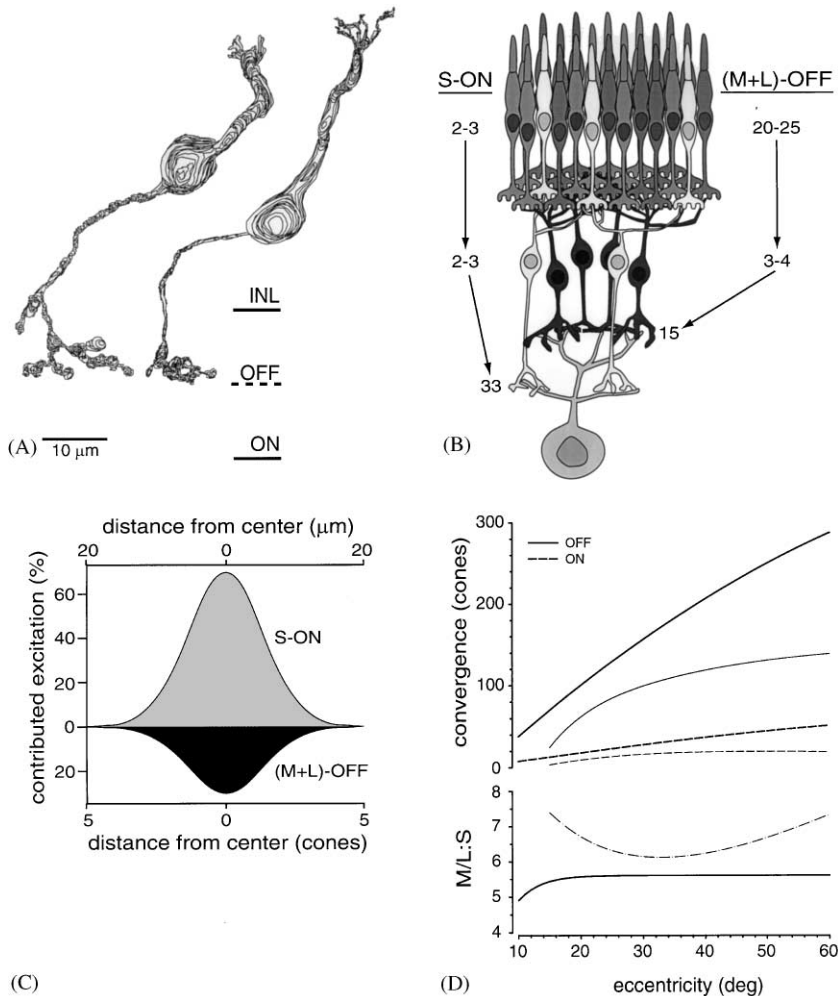


Fig. 15. Circuitry of small bistratified ganglion cell predicts its spatial receptive field. (A) Reconstructions from electron micrographs of DB2 and DB3 diffuse bipolar cells that contact the dendrites of the small bistratified ganglion cell in the OFF stratum of the inner plexiform layer in macaque fovea. These cells are distinguishable by several criteria. INL: inner nuclear layer. (B) Summary of the pre-synaptic circuitry of the small bistratified ganglion cell in macaque fovea. The ganglion cell collects mostly from one S cone via 33 synapses from 2–3 S bipolar cells (light) and from 20–25 M and L cones via 15 synapses from 3–4 DB2 and DB3 cells (dark). (C) Estimated receptive field of the ganglion cell contains spatially co-extensive regions excited by onset of S-cone stimuli (light region) and offset of M- and L-cone stimuli (dark region). The S-ON region represents the receptive field of a single S cone. This was modeled as a Gaussian point spread with a full width at half-height of 2.7 cones, based on a cutoff frequency of 7–14 c/d for optical modulation of short wavelengths (Williams *et al.*, 1993; Marimont and Wandell, 1994) and for S cone-mediated acuity (Fig. 6B). Its amplitude was set by the percentage of excitatory synapses contributed to the ganglion cell by S bipolar cells (70%). The (M+L)-OFF region represents the receptive field of a patch of 20 M and L cones. The amplitude of the smoothed sum from this patch was set by the percentage of excitatory synapses contributed by diffuse OFF bipolar cells (30%). Details in Calkins *et al.* (1998). (D) Top: convergence of M/L cones to the OFF dendritic tree and of S cones to the ON dendritic tree of the small bistratified ganglion cell in human (thick lines) and macaque (thin lines) retina. Convergence calculated as the product of dendritic tree area (polynomials in Fig. 9) with average density of S cones (from Figs. 6A and 7A) or of M/L cones (from Curcio *et al.*, 1990). Bottom: ratio of convergence of M/L cones to S cones in human (stippled trace) and macaque (solid trace) retina. The ratios are nearly constant across retinal eccentricity.

may also explain the faster time to peak for the S component (Chichilnisky and Baylor, 1999; Sterling, 1999).

The diameter of the dendritic arbor of the small bistratified cell in the OFF stratum is systematically about 75% that of the corresponding ON

arbor (Fig. 14A; Dacey, 1993). The area encompassed by the OFF tree reflects this difference accordingly (Fig. 9). Nevertheless, because of their greater density, the estimated convergence of M and L cones is much higher than the convergence of S cones. In the macaque fovea, 20–25 M and L cones converge on the ganglion cell (Fig. 15B). This convergence is systematically about 5-fold higher across the human retina and 6- or 7-fold higher across most of the macaque retina (Fig. 15D).

#### 4.6. Setting the neutral point for the S-ON/(M+L)-OFF receptive field

The computed S-ON/(M+L)-OFF receptive field in Fig. 15C demonstrates that the great width of the spatial aperture of the S cone itself, combined with synaptic weighting, effectively molds the S-ON component into a continuous, smooth profile (see also Sterling, 1999). Thus, the spatial and spectral response profiles of the S-ON/(M+L)-OFF ganglion cell are consistent with cells involved in blue/yellow opponency. Interestingly, the ratio of the convergence of M/L cones to S cones remains roughly constant over retinal eccentricity (Fig. 15D). Other factors aside, this consistency would contribute to a more or less uniform spectral neutral point of S-ON/(M+L)-OFF cells. Certainly in the narrow range of eccentricities tested in the macaque retina, this is so (Zrenner, 1983). Similarly, the neutral point of the blue/yellow channel in human observers is also remarkably uniform across a wide range of eccentricities (see Fig. 6 in Hibino, 1992). The relative number of M versus L cones likely depends upon eccentricity in the human retina (Hagstrom *et al.*, 1998). It would be interesting to determine whether the synaptic weights of the S and M/L components of the ganglion cell receptive field change to accommodate the M:L ratio.

On the other hand, the computed S-ON/(M+L)-OFF receptive field in Fig. 15C is based solely on converging excitation from bipolar cell circuits. In fact, two levels of inhibition also contribute to the circuitry of the ganglion cell. In the inner plexiform layer, amacrine cells provide numerous synapses to the ganglion cell dendritic tree (Dacey, 1993; Calkins *et al.*, 1998; Ghosh and

Grünert, 1999), while in the outer plexiform layer, horizontal cells provide a feedback signal to cones proportional to their mean activity (Sterling, 1999). Both levels of inhibition could contribute to a surround mechanism for the bipolar cells (Dacey, 1999). In particular, the H1 horizontal cell collects signals almost exclusively from M and L cones and lacks any substantial contact with S cones, while the H2 horizontal cell collects from and can provide feedback to all three cone types (Dacey *et al.*, 1996; Goodchild *et al.*, 1996; Chan and Grünert, 1998; Dacey *et al.*, 2000). Thus, both H1 and H2 cells would be able to contribute to the surround of the DB2 and DB3 bipolar cells, while the H2 cell could contribute to the surround for the S bipolar cell (for review, see Martin, 1998). Nevertheless, the ganglion cell apparently lacks a surround mechanism altogether, and changing the size of a stimulus centered on the receptive field modifies very little the net response of the cell (Wiesel and Hubel, 1966; de Monasterio, 1978). One simple explanation for this is that the net reduction in activity in the OFF and ON bipolar pathways via horizontal cell feedback is about equivalent because of the overwhelming preponderance of input from M and L cones to both H1 and H2 cells (Rodieck, 1998).

#### 4.7. Conservation of the S cone and its pathways

The absence of trichromacy, i.e., the absence of two photopigments in the M/L range, is often misconstrued as total color blindness, that is, as the inability to discriminate surfaces based on spectral reflectance alone. Thus, often it has been said that among the mammals, primates alone possess “color vision” (see the discussion in Jacobs, 1993). However, this is simply not the case, as the presence of any two photopigments opens up at least the possibility of using the difference between their spectral absorptions as a basis for color discrimination. Indeed most mammals are nominal dichromats, possessing an S cone and a second cone type with peak sensitivity somewhere in the middle wavelength range of 500–565 nm (Jacobs, 1993). If in fact the S cone begins a common pathway for blue/yellow color discrimination that is truly conserved across mammalian species/orders, then such a system ought to

bear certain strong similarities with the Old World system described in this review. Certainly, the most salient of these features is convergence of antagonistic signals between cone types, e.g., S/(M). For some non-primate mammals, such antagonism is clearly demonstrable in spectral sensitivity or neutral point measurements (dog: Neitz *et al.*, 1989; ground squirrel: Jacobs, 1993; wallaby: Hemmi, 1999). These psychophysical measurements imply that the post-synaptic circuitry of the S cone that underlies this nominal blue/yellow opponency is also likely conserved across species. Certainly this is the case in the New World marmoset, where careful anatomical studies have demonstrated connectivity similar to that in the macaque retina for the S cone bipolar cell, the H2 horizontal cell, and the small bistratified ganglion cell (Chan and Grünert, 1998; Ghosh *et al.*, 1997; Ghosh and Grünert, 1999; Luo *et al.*, 1999). Thus, for good reason, others have called the S cone and the neurons associated with its signals the “primordial subsystem” (Mollon, 1989). Conversely, where the S cone is missing, as in the New World owl monkey, so too apparently are the retinal inter-neurons and central projections that could otherwise underlie the discrimination of blue from yellow (reviewed in Kremers *et al.*, 1999).

## 5. SIGNALS FROM S CONES TO OTHER NEURAL PATHWAYS

The robustness of the data linking the anatomical circuitry of the small bistratified ganglion cell to the S-ON/(M+L)-OFF receptive field has reinforced the association of S cones with a single perceptual channel for color. Vision with S cones is generally linked with poor temporal resolution (e.g., Pugh and Mollon, 1979; Wisowaty and Boynton, 1980; Kelly, 1983), and certainly the chromatic channels are relatively sluggish. However, even a cursory review of the psychophysical literature commends a more conservative view. For example, if one considers whether S cones contribute to an achromatic, luminance channel, the answer very much depends on how one defines “luminance” operationally, an issue that is quite beyond the scope of this review and is taken up

elsewhere (Lennie *et al.*, 1993). Along these lines, under conditions that may or may not tap a chromatic channel, S cones can follow rapidly flickering stimuli (Stockman *et al.*, 1991;1993) and can contribute to motion perception (Cavanagh *et al.*, 1984; Lee and Stromeyer, 1989; Dougherty *et al.*, 1999) and binocular rivalry (O’Shea and Williams, 1996). These tasks generally are associated with a luminance channel. The nature of this S input, or whether signals from S cones are revealed at all in a particular task, depends greatly upon the particular configuration of the stimulus (Eisner and Macleod, 1980; Lennie and D’Zmura, 1988; Shinomori *et al.*, 1999). Nevertheless, S cones are generally depicted as “skipping” contact with additional post-synaptic pathways (e.g., Martin, 1998).

### 5.1. An S signal for motion

Our ability to discriminate the direction of motion is certainly impaired, but not entirely absent, for red/green chromatic stimuli (for review, see Gegenfurtner and Hawken, 1996). This implies that somewhere in the visual pathways, the color difference signal from M and L cones is utilized for motion processing. Neurons of the middle temporal area of the visual cortex (MT) are selective for the direction and speed of moving stimuli, and damage to MT dramatically impairs motion discrimination (for review, see Croner and Albright, 1999). These same neurons also respond to the motion of red/green patterns, albeit more weakly than to achromatic patterns (Dobkins and Albright, 1994; Gegenfurtner *et al.*, 1994). Gegenfurtner *et al.*, however, reported little, if any, S input to directionally selective neurons in area MT. This result seemingly parallels geniculate and retinal ganglion cell recordings that demonstrate a lack of significant S signals in the cells forming the pathway that provides a major input to area MT (Gouras, 1968; Lee *et al.*, 1988; Dacey and Lee, 1994).

On the other hand, experiments in which observers use chromatic stimuli to either cancel luminance motion or match the motion of cone-isolating stimuli have provided strong evidence that S cones do indeed contribute, at some level, to the same motion pathway as M and L cones,

although more weakly (Cavanagh and Anstis, 1991; Chichilnisky *et al.*, 1993; Dougherty *et al.*, 1999). Similarly, imaging studies of human cortex activated by S-cone isolating stimuli show strong input not only to primary visual cortex (as expected), but also to the cortical motion area “MT+” (Wandell *et al.*, 1999). These results are backed by highly sensitive multi-cell recordings from macaque MT that demonstrate unequivocal S input to directionally selective neurons (Seidemann *et al.*, 1999; reviewed in Dobkins, 2000). Thus, the question seems to be no longer whether signals from S cones are utilized for tasks aside from blue/yellow discrimination, but how those signals reach where they are going.

The popular consensus seems to be that S signals find their way to MT via the same pathway used by the S-ON/(M+L)-OFF ganglion cells (reviewed in Dobkins, 2000). Recordings of S-ON/(M+L)-OFF responses with subsequent back-filling of ganglion cells and retrograde labeling from the geniculate indicate that the small bistratified ganglion cell projects to the intermediate “koniocellular” populations nestled within the parvocellular geniculate (Martin *et al.*, 1997; Hendry and Calkins, 1998; Hendry and Reid, 2000). So the working hypothesis is that the S input to MT is through the small bistratified ganglion cell via a circuit originating in the koniocellular geniculate pathway. Such a circuit would provide a basis for mixing signals used for blue/yellow color vision with signals used for motion discrimination. If so, then one ought to be able to cancel the S input to the motion channel by silencing the S-ON/(M+L)-OFF pathway early on with appropriately chosen equilibrium lights.

Perhaps a more parsimonious explanation would be that the S signals simply “piggyback” their way to MT along the same pathway used by M and L cones through a common retinal circuit. Additional cortical connections would not be needed, and the retina need not distinguish between the three types of cone in forming its synaptic connections. The source of what ultimately becomes a motion signal in MT is thought to be a neural pathway that begins with large-field, “parasol” ganglion cells that project to primary

visual cortex via the magnocellular region of the geniculate (reviewed in Kaplan *et al.*, 1990; Merigan and Maunsell, 1993; Lee, 1996; Rodieck, 1998). Both the ganglion cells and the geniculate cells in this pathway have receptive field centers broadly tuned to wavelength and respond phasically to light.

One question to ask, then, is whether there is clear evidence for S input to this canonical magnocellular pathway. This is a difficult issue to resolve, primarily because studies of magnocellular neurons and their retinal counterparts focus almost entirely on responses to “red/green” modulation without using S-isolating stimuli. Where wavelength sensitivity was measured, the cells’ broad-band response would make it difficult in post hoc analysis to tease S from M signals, especially if the S signal is relatively weak (e.g., Wiesel and Hubel, 1966; de Monasterio and Schein, 1980). The few intracellular recordings from morphologically identified parasol cells have not revealed a strong S input (Dacey and Lee, 1994), and these recordings are often cited as support for a single S pathway. On the other hand, in extracellular recordings, phasic ganglion cells with nominally broad-band spectral sensitivity generally have shown fairly strong responses to short wavelengths, consistent with S input (de Monasterio and Gouras, 1975), and selective adaptation has revealed S input to geniculate cells that otherwise would be masked by overwhelming M and L input (Padmos and Norren, 1975). Careful measurements of the spectral characteristics of neurons in the magnocellular region of the geniculate reveal both cells with S-ON and cells with S-OFF responses that oppose a net signal from M and L cones (Derrington *et al.*, 1984). However, given the robustness of the response of the H2 horizontal cell to modulation of S cones (Dacey *et al.*, 1996), it is not clear whether this net S signal originates in the center or surround. Moreover, given the presence of two robust koniocellular populations in the ventral-most geniculate (reviewed in Hendry and Calkins, 1998), the possibility that neurons with S input and nominally “magnocellular” properties are actually koniocellular must be considered. If and how these neurons could contribute to motion discrimination is not known.

## 5.2. Connections from S cones to other ON circuits

Based on physiology alone, there is little evidence sufficiently strong to refute the hypothesis that neurons forming the magnocellular pathway collect excitatory signals from S cones: the spectral measurements are dominated by M and L cones and systematic spectral measurements of the isolated receptive field center are scarce. What insight does the anatomy confer? The synaptic active zone at the axon terminal of the S cone, like that of all photoreceptors, is marked by an electron-dense “ribbon” that points between a pair of horizontal cell processes (both likely to be H2 cells) to an invagination of the terminal membrane. Glutamate diffuses from the ribbon into the invagination and beyond to the post-synaptic cleft of axon terminal. For each ribbon, there are 1–3 central dendrites that penetrate the invagination (reviewed in Calkins, 2000). In primate retina, each invaginating dendrite invariably arises from a nominal ON bipolar cell and expresses the mGluR6 receptor (Fig. 12; Morigiwa and Vardi, 1999; Vardi *et al.*, 2000).

If S cones access a single pathway, then one would expect each invaginating dendrite at an S cone to arise from an S bipolar cell. The other candidates would be the single-cone, “midget” ON bipolar cell and the various types of diffuse ON bipolar (Boycott and Wässle, 1999). Careful reconstructions of the midget pathways in the macaque fovea demonstrate, however, that while each and every M and L cone contacts both a midget ON and midget OFF bipolar cell, the S cone skips any sort of contact with a midget ON cell (Klug *et al.*, 1992, 1993; Herr *et al.*, 1996). The initial impression from tracing the thin dendrites of a diffuse ON bipolar cell *forward* through the outer retina was that they skipped beneath the S cone without contact (Calkins *et al.*, 1996). However, these tracings were incomplete, for they

did not include working *backward* from the invaginations of the S cone. A more thorough taxonomy of all the bipolar cell dendrites penetrating an S cone indicates that this same diffuse ON bipolar cell does contribute a few invaginating dendrites (Table 6, Fig. 16A). In this sense, the S cone terminal is very much like an M or L cone terminal, where diffuse ON bipolar cells also contribute a small number of invaginating dendrites (Fig. 16B). The same diffuse ON bipolar cell that contributes an invaginating dendrite to the S cone in Fig. 16A also forms numerous “semi-invaginating” contacts with the S cone, as it does with neighboring M and L cones (Fig. 16C). These points of contact occur along the wall of the invagination, adjacent to the central, invaginating dendrite, and represent the most frequent site of contact between foveal cones and diffuse ON bipolar cells (Calkins *et al.*, 1996). Thus, based on these contacts, S cones ought to send small depolarizing signals to other ganglion cells via one or more types of diffuse ON bipolar cell. Indeed there are numerous examples of ganglion cells and geniculate cells with S-ON input to their centers with receptive fields that structural differ from the spatially coextensive S-ON and (M+L)-OFF regions of the small bistratified cell (Wiesel and Hubel, 1966; de Monasterio and Gouras, 1975; Dreher *et al.*, 1976).

## 5.3. Connections from S cones to OFF circuits

The parasol OFF cell derives excitatory input via synaptic connections from axon terminals of the DB2 and DB3 diffuse bipolar cells (Calkins, 1999; Jacoby and Marshak, 2000; Jacoby *et al.*, 2000), the same cells that contribute the (M+L)-OFF circuit to the small bistratified ganglion cell. The dendrites of the DB2 and DB3 cells in turn abut the membrane of the cone terminal at sites of “basal” contact that presumably convey the

Table 6. Central dendrites at an S cone<sup>a</sup>

S Cone	Post-synaptic invaginating dendrites		
	Total	S ON	Diffuse ON
Ribbons 26	35	33	2

<sup>a</sup>Modified from Calkins (2000).

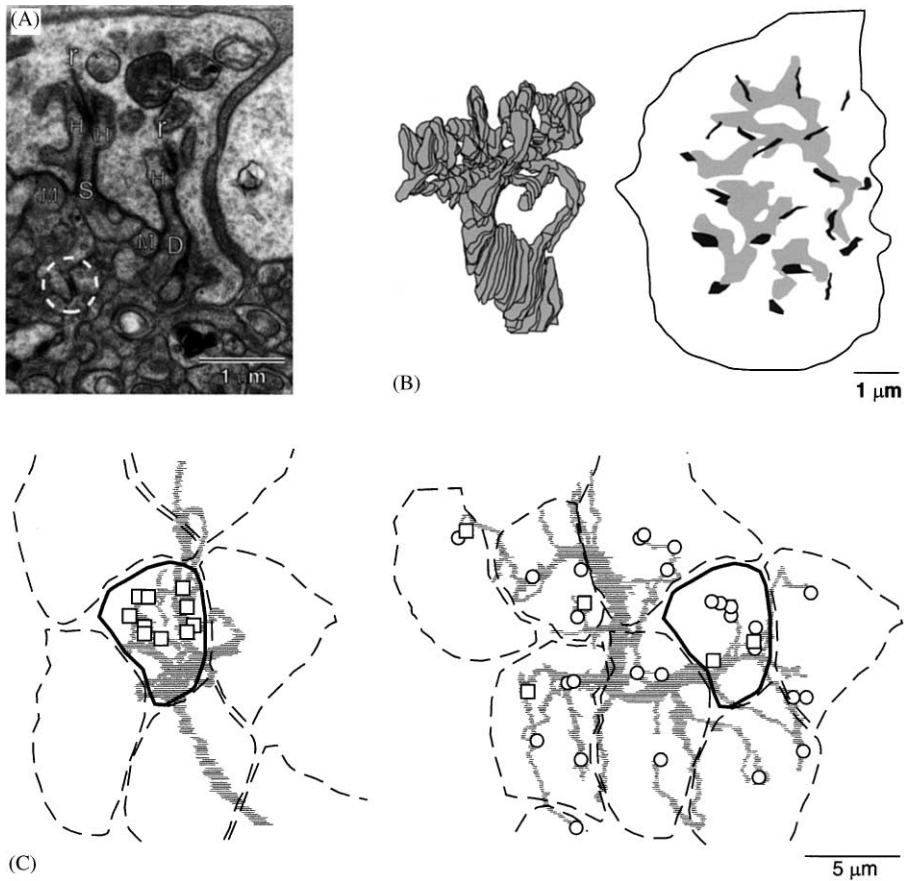


Fig. 16. Divergence from the S cone. (A) Electron micrograph of the axon terminal of an S cone that contacts the small bistratified ganglion cell circuit in Fig. 11D. Glutamate diffuses from pre-synaptic active zones marked by “ribbons” (r) that point between a pair of horizontal cell processes (H) to an invagination of the terminal membrane. Most dendrites that penetrate an invagination centrally arise from S bipolar cells (S), but one or two at each S cone arise from diffuse ON bipolar cells (D). The S cone also contacts a midget OFF bipolar cell (M) at basal positions adjacent to the central dendrite of each invagination. Horizontal cell processes are coupled in the post-synaptic cleft via tiny gap junctions (circle). Electron micrograph from D. Calkins, unpublished. (B) Reconstruction of a midget ON bipolar cell (left) from a neighboring M or L cone, shown in tangential view (right). In contrast to the S cone, the invaginating dendrites at each ribbon (black structures) arise from the midget ON bipolar cell (grey processes). (C) Left: tangential view of the reconstructed S cone terminal in (A) (dark outline). The S bipolar cell whose dendrite is marked by S in (A) (grey profile) contributes 16 invaginating dendrites (squares, some hidden, cell 1 in Table 5). Other dendrites course beneath M and L cones to collect synapses from two additional S cones (not shown). Right: reconstruction of the dendritic tree of a diffuse ON bipolar cell whose dendrites receive contact from the same S cone at two invaginations (squares), but also at numerous “semi-invaginating” or “triad-associated” basal sites along the wall of the invagination (circles). The cell collects most of its synapses from M and L cones (dotted profiles). (B and C) modified from Calkins *et al.* (1996, 1998) and from Calkins (2000).

excitatory signal at light offset (see Section 4.5). From these sites, S cones could conceivably drive the parasol OFF cell via DB2 and DB3. Once again, however, the view stemming from the broad-band spectral response of the magnocellular pathway has been that S cones simply do not contact the diffuse bipolar cells and so cannot provide a signal to the magnocellular pathway

(reviewed in Martin, 1998). This view mandates a strong and wonderfully testable hypothesis to unite the physiology and anatomy in much the same way the synaptic contacts of the H2 horizontal cell with S cones match its spectral response (see Section 4.6). Simply stated, if S cones avoid diffuse OFF bipolar cells, then their post-synaptic space ought to be devoid of any basal

dendrites. In this respect, the axon terminal of the S cone would look like the spherule of the rod, whose only contacts to bipolar cells are invaginating.

Yet, any investigator who has used either morphological or neurochemical means to identify S cones recognizes that the axon terminal of the S cone provides numerous points of basal contact with a large complement of bipolar cell dendrites (Kouyama and Marshak, 1992; Kolb *et al.*, 1997; Calkins *et al.*, 1998; Calkins, 2000). Indeed some of these dendrites are traceable to the DB3 bipolar cell (Calkins, 2000). These basal contacts are relatively rare (Calkins, 2000) and suggest that some parasol OFF ganglion cells should hyperpolarize not only to stimulation of M and L cones, but also weakly to S cones. That such responses are not obvious probably reflects a sampling problem: since S cones are scarce, M and L cones must provide the majority of synapses to diffuse bipolar cells, and only careful isolation of S cones would reveal any, albeit weak, input to nominally “broad-band” ganglion cells (e.g., de Monasterio and Gouras, 1975; Padmos and Norren, 1975).

On the other hand, there are numerous physiological recordings from neurons that derive a pure, S-OFF response (Table 7), and certain psychophysical experiments support S input to OFF channels (most recently, Shinomori *et al.*, 1999; McLellan and Eskew, 2000). The physiological examples are relatively rare, compared to the S-ON/(M+L)-OFF cell, but nonetheless persist across multiple decades of investigation. These studies converge upon two distinct profiles of receptive field. The first very much resembles the S-ON cell, in that the S-OFF response is spatially co-extensive with an (M+L)-ON response. The

second resembles the textbook “red/green” opponent cell, in that the S-OFF response is localized to a center spatially concentric with a mixed M+L surround.

What do these cells do? Complementary ON and OFF mosaics for a particular type of ganglion cell effectively partition the dynamic range of the pathway about the mean light level. Thus, each ganglion cell can utilize the full range of its spiking capacity to signal with excitation either graded increments or decrements from the mean. If such a strategy is used by the color channels, one might expect the ganglion cell with spatially co-extensive S-OFF and (M+L)-ON regions to contribute to the blue/yellow opponent channel (Zrenner, 1983). To make this argument convincing, though, requires identification of its morphological substrate and demonstration that its pre-synaptic circuitry optimizes a spectral signal at the price of spatial information (Calkins and Sterling, 1999). One possible candidate is a ganglion cell whose dendrites collect synapses from the S bipolar cell not at the axon terminal, but at ribbons located in the descending axon itself within the OFF region of the inner plexiform layer (Fig. 6B in Calkins *et al.*, 1998) These contacts could supply the ganglion cell with a pure S signal.

The cell with spatially concentric S-OFF center and (M+L)-ON surround may be simpler to explain. Each M and L cone over much of the primate retina contacts a single midget ON and a single midget OFF bipolar cell (Calkins *et al.*, 1994; Wässle *et al.*, 1994), and this circuit underlies the spatial antagonism necessary for acuity (reviewed in Calkins and Sterling, 1999). Similarly, while the S cone lacks a midget ON bipolar cell (see Section 5.2), it does contact a midget OFF

Table 7. S-OFF cells in primate extracellular recordings<sup>a</sup>

Spectral profile	Spatial profile	Structure	Refs.
S-OFF/(M+L)-ON	Co-extensive	Parvocellular LGN Retina	1–3 4,5
S-OFF/(M+L)-ON	Concentric	Parvocellular LGN Retina	1,6 4
S-OFF/(M+L)-ON	—	Parvocellular LGN	7–9

<sup>a</sup> Refs.: (1) Wiesel and Hubel (1966); (2) Dreher *et al.* (1976); (3) Valberg *et al.* (1986); (4) de Monasterio and Gouras (1975); (5) Zrenner and Gouras (1981); (6) Krüger (1977); (7) De Valois *et al.* (1966); (8) Marroco (1976); (9) Derrington *et al.* (1984).

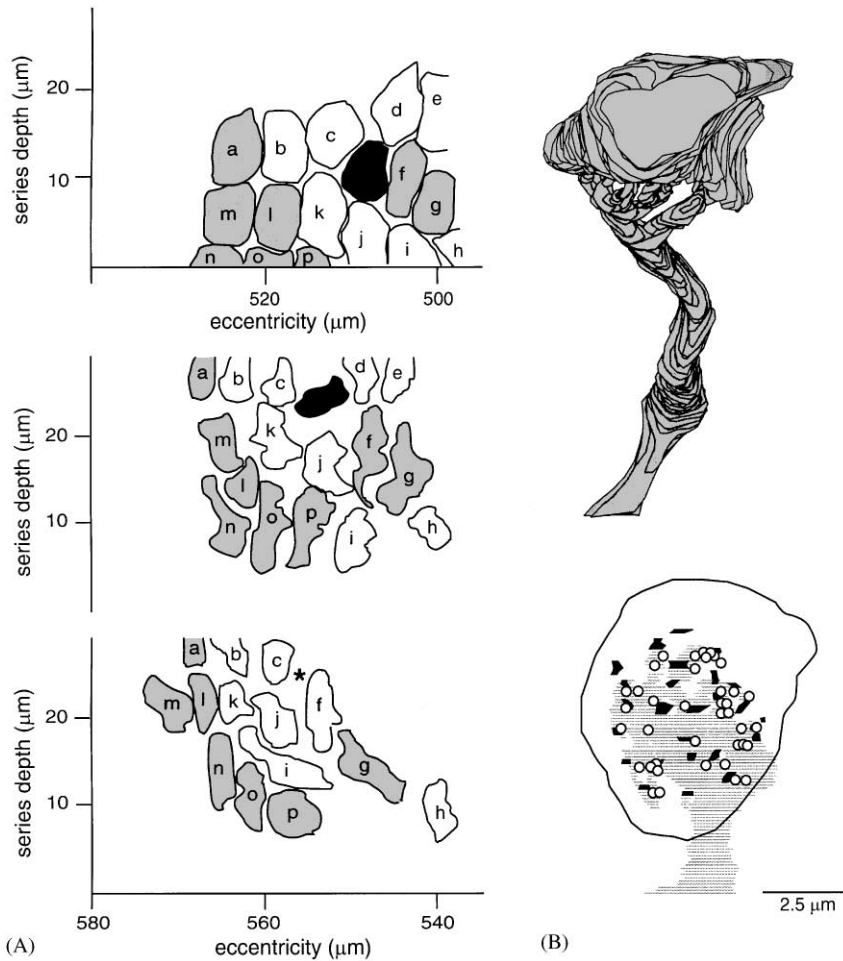


Fig. 17. S cones contact an OFF midget bipolar cell. (A) Top: tangential view of reconstructions from electron micrographs of a few neighboring cone axon terminals in macaque fovea. Some cones (white) contacted midget ON and OFF pathways with about 30 bipolar  $\rightarrow$  ganglion cell synapses, while others (grey) contacted midget ON and OFF pathways with about 50 bipolar  $\rightarrow$  ganglion cell synapses (see Calkins *et al.*, 1994). The S cone in Fig. 16B and C is in this patch (black). Middle: from the inner plexiform layer, outlines of the axonal terminals of the midget OFF bipolar cells from the same patch of cone terminals, including the S cone (black). Bottom: outlines of the axonal terminals of the midget ON bipolar cells from the same patch of cones. All but the S cone contact a midget ON cell (asterisk marks the "empty" space). Modified from Calkins (1999). (B) Top: reconstruction from electron micrographs of the axon terminal of the S cone in A (light traces) contacting the dendritic tree of its midget OFF bipolar cell (darker traces). Bottom: tangential view of the cone terminal (outline), its ribbon synapses (black structures), and the locations of contact (circles) to the dendritic tree of the bipolar cell (grey profile). These contacts occur invariably at "semi-invaginating" or "triad-associated" basal sites along the wall of each invagination the cone terminal. Reconstructions from D. Calkins, unpublished.

bipolar cell (Fig. 17), and this cell apparently contacts a single midget ganglion cell (Klug *et al.*, 1992, 1993). Presumably the spatial structure of its receptive field is similar to those of other midget cells, though we might expect a broader S center due to blurring (as in Fig. 1). What is lacking here is a demonstration that this circuit forms a regular mosaic across the retina and, therefore, can

contribute in a meaningful way to a psychophysical channel.

## 6. SUMMARY: A LESSON IN EVOLUTION

The study of the S cone, its mosaic and post-synaptic pathways is a study of evolutionary

pressures and how they work to shape the connectivity and sampling properties of a visual circuit. The S cone is rare, sampling only as necessary to match the spatial distribution of contrast the optics of the eye affords (Section 2.1). In the human eye, at the central retinal location where these optics blur the focal point of short wavelength light under standard accommodation, the S cone is missing. In other primates, the smaller the eye, the better the optics and the smaller this S-free zone (Section 3.2). A comparison of the post-synaptic pathways of the S cone with psychophysical measures of S-mediated vision offers other insights into how evolutionary pressures might have shaped the architecture of the circuits that collect S signals and send them to the brain.

### 6.1. A circuit for color vision

The strength of psychophysical studies of the S cone rests on the capacity to isolate its signals from the other photoreceptors, through selective adaptation. The data summarized in this review lay a rather parsimonious framework for linking psychophysical work that exploits this separability with a particular retinal circuit and retinogeniculate pathway. Acuity tests using stimuli that isolate the S cone indicate that whichever psychophysical channel is tapped in these tests, its spatial frequency range is matched by the sampling rate of the S cone (Fig. 6). It is not clear that these acuity tests uniformly and unequivocally isolate the canonical blue/yellow opponent channel, indeed to suppose so without an independent test of opponency is to equate seeing with S cones with this single perceptual channel.

A retinal circuit optimized for color should compare spectral signals at the cost of spatial information (Calkins and Sterling, 1999). It is now apparent that the blue/yellow channel has as part of its roots just such a circuit in which signals from S cones are combined antagonistically but co-extensively with signals from M and L cones. The small bistratified ganglion cell that forms the hallmark of this circuit also samples the cone mosaic with frequency sufficient to underlie the acuity tasks: about one for each S cone (Section 4.2). In this sense, the small bistratified cell is like

the “P” or “midget” ganglion cell, whose ON and OFF mosaics in the central retina both match in density the mosaic of M and L cones (reviewed in Calkins and Sterling, 1999). However, even in the fovea, where the midget cell collects excitatory input only from a single cone (Calkins *et al.*, 1994), the small bistratified cell collects from several S cones. Despite this convergence, the circuitry of the cell is such that one of these S cones predominates in providing synaptic input to the ganglion cell. This is so over the entire retina (Section 4.4). Thus, the ganglion cell is able to serve two evolutionary pressures at once: to improve its sensitivity and the integrity of its signal through convergence, while also preserving the spatial resolution of the neural image of the S mosaic. What remains now is a better understanding of how the excitatory elements of the ganglion cell’s circuit (the ON and OFF bipolar cells) combine with the inhibitory elements (amacrine and horizontal cells) to produce the net antagonism that so resembles that of the blue/yellow channel.

### 6.2. The S cone and other circuits

The robustness of the hypothesis that links the small bistratified ganglion cell with blue/yellow color vision in some ways is tied to the frequency and consistency with which its S-ON/(M+L)-OFF receptive field is mapped physiologically. That other physiological types are apparently less common has bolstered the idea that signals from S cones traverse a single pathway from the retina to the brain (Section 5.1). Thus, based on this idea, any mixing of S signals with other perceptual channels, such as a motion channel, must occur somewhere in the cortical milieu (Dobkins, 2000). Yet, it is recognized that even for blue/yellow color vision another ganglion cell with the opposite spectral signature (i.e., (M+L)-ON/S-OFF) is likely necessary to complete the channel (Zrenner, 1983). Though rare, the physiological literature holds examples of such a cell (Section 5.3), and there is growing psychophysical support for S input to OFF channels (Shinomori *et al.*, 1999).

Certainly, that the physiological receptive field in which S-ON and (M+L)-OFF signals converge co-extensively is now linked unequivocally with an

iterative and highly conserved anatomical circuit has raised the bar considerably for what is considered ample evidence for the existence of a cell “type” (Dacey and Lee, 1994). This is as it should be, as often physiological “types” disappear with more detailed and quantitative scrutiny (see Calkins and Sterling, 1999). On the other hand, the devil is in the details, and quantitative anatomy often reveals a great many details that — for the time being — simply are beyond the resolution of other tools, either because of sampling or some other form of bias. With other types of receptive field with S input sprinkled throughout the literature, it may be that the preliminary anatomical indications of divergence from the S cone to other bipolar cell → ganglion cell circuits will indeed map with consistency to distinct physiological types with further exploration (Sections 5.2 and 5.3). What is required is a systematic study of the post-synaptic space of the S cone across retinal eccentricity, coupled with a careful analysis of the spatial structure of ganglion cell receptive fields under conditions intended to exploit even the weakest of signals from S cones.

*Acknowledgements*—I thank the members of my laboratory for their contributions to the Figs. contained in this paper: T. McDaniel, K. Jensen and D. Sanchez. I also thank P. Sterling and S. Hendry for their energetic and generous collaborations and J. Nathans, A. Szél, N. Vardi and J. Del Valle for donating antibodies. Professors Brian Wandell of Stanford University and David Williams of the University of Rochester read and improved the manuscript tremendously with their comments. This work was supported by grants from the National Eye Institute (EY 12480), the Sloan Foundation and Research to Prevent Blindness.

## REFERENCES

- Ahnelt, P., Kolb, H. and Pflug, R. (1987) Identification of a subtype of cone photoreceptor, likely to be blue sensitive, in the human retina. *J. Comp. Neurol.* **255**, 18–34.
- Ahnelt, P., Keri, C. and Kolb, H. (1990) Identification of pedicles of putative blue-sensitive cones in the human retina. *J. Comp. Neurol.* **293**, 39–53.
- Baylor, D. A., Nunn, B. J. and Schnapf, J. L. (1987) Spectral sensitivity of cones of the monkey *Macaca fascicularis*. *J. Physiol.* **390**, 145–160.
- Bowmaker, J. K., Astell, S., Hunt, D. M. and Mollon, J. D. (1991) Photosensitive and photostable pigments in the retinae of old world monkeys. *J. Exp. Biol.* **156**, 1–19.
- Boycott, B. B. and Wässle, H. (1999) Parallel processing in the mammalian retina. The proctor lecture. *Inv. Ophthalm. Vis. Sci.* **40**, 1313–1327.
- Brainard, D. H. and Williams, D. R. (1993) Spatial reconstruction of signals from short-wavelength cones. *Vision Res.* **33**, 105–116.
- Buchsbaum, G. and Gottschalk, A. (1983) Trichromacy, opponent colors coding and optimum color information transmission in the retina. *Proc. R. Soc. (Lond.) B* **220**, 89–113.
- Bumsted, K. and Hendrickson, A. (1999) Distribution and development of short-wavelength cones differ between *Macaca* monkey and human fovea. *J. Comp. Neurol.* **403**, 502–516.
- Calkins, D. J. (1999) Synaptic organization of cone pathways in the primate retina. In *Color vision: from molecular genetics to perception* (eds. K. Gegenfurtner and L. Sharpe), Cambridge University Press, Cambridge.
- Calkins, D. J. (2000) The representation of cone signals in the primate retina. *J. Opt. Soc. Am. A.* **17**, 597–606.
- Calkins, D. J. and Sterling, P. (1999) Evidence that circuits for spatial and opponent color vision segregate at the first retinal synapse. *Neuron* **24**, 313–321.
- Calkins, D. J., Tsukamoto, Y. and Sterling, P. (1996) Foveal cones form basal as well as invaginating junctions with diffuse ON bipolar cells. *Vision Res.* **36**, 3373–3381.
- Calkins, D. J., Tsukamoto, Y. and Sterling, P. (1998) Microcircuitry and mosaic of a blue/yellow ganglion cell in the primate retina. *J. Neurosci.* **18**, 3373–3385.
- Calkins, D. J., Schein, S., Tsukamoto, Y. and Sterling, P. (1994) M and L cones in Macaque fovea connect to midget ganglion cells via different numbers of excitatory synapses. *Nature* **371**, 70–72.
- Cavanagh, P., Tyler, C. W. and Favreau, O. E. (1984) Perceived velocity of moving chromatic gratings. *J. Opt. Soc. Am. A.* **1**, 893–899.
- Cavanagh, P. and Anstis, S. (1991) The contribution of color to motion in normal and color-deficient observers. *Vision Res.* **31**, 2109–2148.
- Chan, T. L. and Grünert, U. (1998) Horizontal cell connections with short wavelength-sensitive cones in the retina: a comparison between new world and old world primates. *J. Comp. Neurol.* **393**, 196–209.
- Chen, J., Tucker, C. L., Woodford, B., Szél, A., Lem, J., Gianella-Borradori, A., Simon, M. I. and Bogenmann, E. (1994) The human blue opsin promoter directs transgene expression in short-wave cones and bipolar cells in the mouse retina. *Proc. Nat. Acad. Sci. USA* **91**, 2611–2615.
- Chichilnisky, E. J. and Baylor, D. A. (1999) Receptive-field microstructure of blue-yellow ganglion cells in primate retina. *Nature Neurosci.* **2**, 889–893.
- Chichilnisky, E., Heeger, D. J. and Wandell, B. A. (1993) Functional Segregation of Color and Motion Perception Examined in Motion Nulling. *Vision Res.* **33**, 2113–2125.
- Chiu, M. I. and Nathans, J. (1994) A Sequence upstream of the mouse blue visual pigment gene directs blue cone-specific transgene expression in mouse retinas. *Visual Neurosci.* **11**, 773–780.
- Cohen, E. D. and Miller, R. F. (1994) The role of NMDA and non-NMDA excitatory amino acid receptors in the functional organization of primate ganglion cells. *Visual Neurosci.* **11**, 317–332.
- Croner, L. J. and Albright, T. D. (1999) Segmentation by color influences responses of motion-sensitive neurons in the

- cortical middle temporal visual area. *J. Neurosci.* **19**, 3935–3951.
- Curcio, C. A. and Hendrickson, A. E. (1991) Organization and development of the primate photoreceptor mosaic. *Prog. Retinal Eye Res.* **10**, 89–120.
- Curcio, C. A., Sloan, K. R., Kalina, R. E. and Hendrickson, A. E. (1990) Human photoreceptor topography. *J. Comp. Neurol.* **292**, 497–523.
- Curcio, C. A., Allen, K. A., Sloan, K. R., Lerea, C. L., Hurley, J. B., Klock, I. B. and Milam, A. H. (1991) Distribution and morphology of human cone photoreceptors stained with anti-blue opsin. *J. Comp. Neurol.* **312**, 610–624.
- Dacey, D. M. (1993) Morphology of a small field bistratified ganglion cell type in the macaque and human retina. *Visual Neurosci.* **10**, 1081–1098.
- Dacey, D. M. (1996) Circuitry for color coding in the primate retina. *Proc. Natl. Acad. Sci. USA* **93**, 582–588.
- Dacey, D. M. and Lee, B. B. (1994) The 'blue-on' opponent pathway in primate retina originates from a distinct bistratified ganglion cell type. *Nature* **367**, 731–735.
- Dacey, D. M. (1999) Primate retina: cell types, circuits and color opponency. *Prog. Retinal Eye Res.* **18**, 737–763.
- Dacey, D. M., Lee, B. B., Stafford, D. K., Pokorny, J. and Smith, V. C. (1996) Horizontal cells of the primate retina: cone specificity without spectral opponency. *Science* **271**, 656–659.
- Dacey, D. M., Diller, L. C., Verweij, J. and Williams, D. R. (2000) Physiology of L- and M-cone inputs to H1 horizontal cells in the primate retina. *J. Opt. Soc. Am. A* **17**, 589–596.
- Dartnall, H. J. A., Bowmaker, J. K. and Mollon, J. D. (1983) Human visual pigments: microspectrophotometric results from the eyes of seven persons. *Proc. Roy. Soc. Lond.* **220**, 115–130.
- Daw, N. W. and Enoch, J. M. (1973) Contrast sensitivity, Westheimer function and Stiles-Crawford effect in a blue cone monochromat. *Vision Res.* **13**, 1669–1679.
- De Valois, R. L., Abramov, I. and Jacobs, G. H. (1966) Analysis of response patterns of LGN cells. *J. Opt. Soc. Am.* **56**, 966–977.
- Derrico, J. B. and Buchsbaum, G. (1991) A computational model of spatio-chromatic coding in early vision. *J. Visual Communication and Image Representation* **2**, 31–38.
- Derrington, A. M., Krauskopf, J. and Lennie, P. (1984) Chromatic mechanisms in lateral geniculate nucleus of macaque. *J. Physiol.* **357**, 241–265.
- Derrington, A. M. and Lennie, P. (1984) Spatial and temporal contrast sensitivities of neurons in lateral geniculate nucleus of macaque. *J. Physiol.* **357**, 219–240.
- Dobkins, K. R. (2000) Moving colors in the lime light. *Neuron* **25**, 15–18.
- Dobkins, K. R. and Albright, T. D. (1994) What happens if it changes color when it moves? the nature of chromatic input to macaque visual area MT. *J. Neurosci.* **14**, 4854–4870.
- Dougherty, R. F., Press, W. A. and Wandell, B. A. (1999) Perceived speed of colored stimuli. *Neuron* **24**, 893–899.
- Dreher, B., Fukuda, Y. and Rodieck, R. W. (1976) Identification, classification and anatomical segregation of cells with X-like and Y-like properties in the lateral geniculate nucleus of Old-World primates. *J. Physiol.* **258**, 433452.
- Eisner, A. and MacLeod, D. I. A. (1980) Blue sensitive cones do not contribute to luminance. *J. Opt. Soc. Am.* **70**, 121–123.
- Euler, T., Schneider, H. and Wässle, H. (1996) Glutamate responses of bipolar cells in a slice preparation of the rat retina. *J. Neurosci.* **16**, 2934–2944.
- Gegenfurtner, K. R. and Hawken, M. J. (1996) Interaction of Motion and Color in the Visual Pathways. *Trends in Neurosci.* **19**, 394–401.
- Gegenfurtner, K. R., Kiper, D. C., Beusmans, J. M. H., Carandini, M., Zaidi, Q. and Movshon, A. (1994) Chromatic Properties of Neurons in Macaque MT. *Visual Neurosci.* **11**, 445–466.
- Ghosh, K. K. and Grünert, U. (1999) Synaptic input to small bistratified (blue-ON) ganglion cells in the retina of a new world monkey, the marmoset *Callithrix jacchus*. *J. Comp. Neurol.* **413**, 417–428.
- Ghosh, K. K., Martin, P. R. and Grünert, U. (1997) Morphological analysis of the blue cone pathway in the retina of a new world monkey, the marmoset *Callithrix jacchus*. *J. Comp. Neurol.* **379**, 211–225.
- Goodchild, A. K., Chan, T. L. and Grünert, U. (1996) Horizontal cell connections with short-wavelength-sensitive cones in macaque monkey retina. *Visual Neurosci.* **13**, 833–845.
- Gouras, P. (1968) Identification of cone mechanisms in monkey ganglion cells. *J. Physiol.* **199**, 533–547.
- Green, D. G. (1972) Visual acuity in the blue cone monochromat. *J. Physiol.* **196**, 415–429.
- Hagstrom, S. A., Neitz, J. and Neitz, M. (1998) Variations in cone populations for red-green color vision examined by analysis of mRNA. *NeuroReport* **9**, 1963–1967.
- Harosi, F. (1987) Cynomolgus and rhesus monkey visual pigment. *J. Gen. Physiol.* **89**, 717–743.
- Hartveit, E. (1997) Functional organization of cone bipolar cells in the rat retina. *J. Neurophysiol.* **77**, 1726–1730.
- Hemmi, J. M. (1999) Dichromatic color vision in an Australian marsupial, the tammar wallaby. *J. Comp Physiol A* **185**, 509–515.
- Hendrickson, A. E. (1998) Primate foveal development: a microcosm of current questions in neurobiology. *Inv. Ophthalm. Vis. Sci.* **35**, 3129–3133.
- Hendry, S. H. C. and Calkins, D. J. (1998) Neuronal chemistry and functional organization in primate visual system. *Trends in Neurosci.* **21**, 344–349.
- Hendry, S. H. C. and Reid, R. C. (2000) The koniocellular pathway in primate vision. *Annu. Rev. Neurosci.* **23**, 127–153.
- Herr, S. S., Tiv, N., Sterling, P. and Schein, S. J. (1996) S cones in macaque fovea are invaginated by one type of ON bipolar cell, but L and M cones are invaginated by midget and diffuse bipolar cells. *Inv. Ophthalm. Vis. Sci. (Suppl.)* **37**, 4864.
- Hess, R. F., Mullen, K. T. and Zrenner, E. (1989) Human photopic vision with only short wavelength cones post-receptor properties. *J. Physiol.* **417**, 151–172.
- Hibino, H. (1992) Red-green and yellow-blue opponent color responses as a function of retinal eccentricity. *Vision Res.* **32**, 1955–1964.
- Hunt, D. M., Cowing, J. A., Patel, R., Appukuttan, B., Bowmaker, J. K. and Mollon, J. D. (1995) Sequence and evolution of the blue cone pigment gene in old and new world primates. *Genomics* **27**, 535–538.
- Hurvich, L. M. and Jameson, D. (1957) An opponent-process theory of color vision. *Psychol. Rev.* **64**, 384–404.
- Jacobs, G. H. (1993a) The distribution and nature of color vision among the mammals. *Biol. Rev.* **68**, 413–471.

- Jacobs, G. H. (1996) Primate photopigments and primate color vision. *Proc. Natl. Acad. Sci. USA* **93**, 577–581.
- Jacobs, G. H. and Deegan, J. F. (1993b) Photopigments underlying color vision in ringtail lemurs (*Lemur cattaemur catta*) and brown lemurs (*Eulemur fulvus*). *Am. J. Primatology* **30**, 243–256.
- Jacobs, G. H. and Neitz, J. (1986) Spectral mechanisms and color vision in the tree shrew (*Tupaia belangeri*). *Vision Res.* **26**, 291–298.
- Jacoby, R. A. and Marshak, D. W. (2000) Synaptic connections of DB3 diffuse bipolar cell axons in macaque retina. *J. Comp. Neurol.* **416**, 19–29.
- Jacoby, R. A., Wiechmann, A. F., Amara, S. G., Leighton, B. H. and Marshak, D. W. (2000) Diffuse bipolar cells provide input to OFF parasol ganglion cells in the macaque retina. *J. Comp. Neurol.* **416**, 6–18.
- Kaplan, E., Lee, B. B. and Shapley, R. M. (1990) New views of primate retinal function. *Prog. Retinal Eye Res.* **9**, 273–336.
- Kelly, D. H. (1983) Spatiotemporal variation of chromatic and achromatic contrast thresholds. *J. Opt. Soc. Am.* **73**, 742–750.
- Klug, K., Tsukamoto, Y., Sterling, P. and Schein, S. J. (1993) Blue cone off-midget ganglion cells in Macaque. *Inv. Ophthalm. Vis. Sci. (Suppl.)* **34**, 1398.
- Klug, K., Tiv, N., Tsukamoto, Y., Sterling, P. and Schein, S. J. (1992) Blue cones contact OFF-midget bipolar cells. *Soc. Neurosci. Abstract* **19**, 3517.
- Kolb, H., Goede, P., Roberts, S., McDermott, R. and Gouras, P. (1997) Uniqueness of the S-cone pedicle in the human retina and consequences for color processing. *J. Comp. Neurol.* **386**, 443–460.
- Kolb, H., Linberg, K. A. and Fisher, S. K. (1992) Neurons of the human retina: a golgi study. *J. Comp. Neurol.* **318**, 147–187.
- Kouyama, N. and Marshak, D. W. (1992) Bipolar cells specific for blue cones in the Macaque retina. *J. Neurosci.* **12**, 1233–1252.
- Kouyama, N. and Marshak, D. W. (1997) The topographical relationship between two neuronal mosaics in the short wavelength-sensitive system of the primate retina. *Visual Neurosci.* **14**, 159–167.
- Kremers, J., Silveira, L. C. L., Yamada, E. S. and Lee, B. B. (1999) The ecology and evolution of primate color vision. In *Color vision: from molecular genetics to perception* (eds. K. Gegenfurtner and L. Sharpe), pp. 123–142. Cambridge University Press, Cambridge.
- Krüger, J. (1977) Stimulus dependent color specificity of monkey lateral geniculate neurones. *Exp. Brain Res.* **30**, 297–311.
- Larimer, J., Krantz, D. H. and Cicerone, C. M. (1975) Opponent process additivity-II. Yellow/blue equilibria and nonlinear models. *Vision Res.* **15**, 723–731.
- Lee, B. B., Martin, P. R. and Valberg, A. (1988) The physiological basis of heterochromatic flicker photometry demonstrated in the ganglion cells of the macaque retina. *J. Physiol.* **404**, 323–347.
- Lee, B. B. (1996) Receptive field structure in the primate retina. *Vision Res.* **36**, 631–644.
- Lee, J. and Stromeyer, C. F. III. (1989) Contribution of human short-wave cones to luminance and motion detection. *J. Physiol.* **413**, 563–593.
- Lennie, P. and D'Zmura, M. (1988) Mechanisms of color vision. *CRC Critical Rev. Neurobiol.* **3**, 333–400.
- Lennie, P., Pokorny, J. and Smith, V. C. (1993) Luminance. *J. Opt. Soc. Am. A* **10**(6), 1283–1293.
- Lukasiewicz, P. D., Wilson, J. A. and Lawrence, J. E. (1997) AMPA-preferring receptors mediate excitatory synaptic inputs to retinal ganglion cells. *J. Neurophysiol.* **77**, 57–64.
- Luo, X. G., Ghosh, K. K., Martin, P. R. and Grünert, U. (1999) Analysis of two types of cone bipolar cells in the retina of a New World monkey, the marmoset, *Callithrix jacchus*. *Visual Neurosci.* **16**(4), 707–719.
- Marc, R. E. and Sperling, H. G. (1977) Chromatic organization of primate cones. *Science* **196**, 454–456.
- Mariani, A. P. (1984) Bipolar cells in monkey retina selective for the cones likely to be blue-sensitive. *Nature* **308**, 184–186.
- Marimont, D. H. and Wandell, B. A. (1994) Matching color images: the effects of axial chromatic aberration. *J. Opt. Soc. Am. A* **11**(12), 3113–3122.
- Marroco, R. T. (1976) Sustained and transient cells in monkey lateral geniculate nucleus: conduction velocities and response properties. *J. Neurophysiol.* **39**(2), 340–353.
- Marroco, R. T. and De Valois, R. L. (1977) Locus of spectral neutral point in monkey opponent cells depends on stimulus luminance relative to the background. *Brain Res.* **119**, 465–470.
- Martin, P. R. (1998) Color processing in the primate retina: recent progress. *J. Physiol.* **513**[3], 631–638.
- Martin, P. R. and Grünert, U. (1999) Analysis of the Short Wavelength-Sensitive (“Blue”) Cone Mosaic in the Primate Retina: Comparison of New World and Old World Monkeys. *J. Comp. Neurol.* **406**, 1–14.
- Martin, P. R., White, A. J. R., Goodchild, A. K., Wilder, H. D. and Sefton, A. E. (1997) Short communication: evidence that blue-on cells are part of the third geniculocortical pathway in primates. *Eur. J. Neurosci.* **9**, 1336–1541.
- Massey, S. C. (1990) Cell types using glutamate as a neurotransmitter in the vertebrate retina. *Prog. Retinal Eye Res.* **9**, 399–425.
- McLellan, J. S. and Eskew, Jr., R. T. (2000) ON and OFF S-cone pathways have different long-wave cone inputs. *Vision Res.*, in press.
- Merigan, W. H. and Maunsell, J. H. R. (1993) How parallel are the primate visual pathways? *Annu. Rev. Neurosci.* **16**, 369–402.
- Mollon, J. D., Bowmaker, J. K. and Jacobs, G. H. (1984) Variations of color vision in a New World primate can be explained by polymorphism of retinal photopigments. *Proc. Roy. Soc. Lond. B* **222**, 373–399.
- Mollon, J. D. (1989) “Tho’ she kneel’d in that Place where they grew”. *J. Exp. Biol.* **146**, 21–38.
- Mollon, J. D. and Bowmaker, J. K. (1992) The spatial arrangement of cones in the primate fovea. *Nature* **360**, 677–679.
- de Monasterio, F. M. (1978) Properties of ganglion cells with atypical receptive-field organization in retina of macaques. *J. Neurophysiol.* **41**, 1435–1449.
- de Monasterio, F. M. and Gouras, P. (1975) Functional properties of ganglion cells of rhesus monkey retina. *J. Physiol.* **251**, 167–195.
- de Monasterio, F. M. and Schein, S. J. (1980) Protan-like spectral sensitivity of foveal Y ganglion cells of the retina of the macaque monkeys. *J. Physiol.* **299**, 385–396.
- de Monasterio, F. M., McCrane, E. P., Newlander, J. K. and Schein, S. J. (1985) Density profile of blue-sensitive cones

- along the horizontal meridian of Macaque retina. *Inv. Ophthalm. Visual Science* **26**, 289–302.
- Morigiwa, K. and Vardi, N. (1999) Differential expression of ionotropic glutamate receptor subunits in the outer retina. *J. Comp. Neurol.* **405**, 173–184.
- Mullen, K. T. (1985) The contrast sensitivity of human color vision to red-green and blue-yellow chromatic gratings. *J. Physiol.* **359**, 381–400.
- Myers, K. J., Ingling, Jr., C. R., and Drum, B. A. (1973) Brightness additivity for a grating target. *Vision Res.* **13**, 1165–1173.
- Nakajima, Y., Iwakabe, H., Akazawa, C., Nawa, H., Shigemoto, R., Mizuno, N. and Nakanishi, S. (1993) Molecular characterization of a novel retinal metabotropic glutamate receptor mGluR6 with a high agonist selectivity for L-2-amino-4-phosphonobutyrate. *J. Biol. Chem.* **268**, 11868–11873.
- Nathans, J., Thomas, D. and Hogness, D. S. (1986) Molecular genetics of human color vision: The genes encoding blue, green, and red pigments. *Science* **232**, 193–210.
- Neitz, J., Geist, T. and Jacobs, G. H. (1989) Color vision in the dog. *Visual Neurosci.* **3**, 119–125.
- Noorlander, C., Koenderink, J. J., Den Ouden, R. J. and Edens, B. W. (1983) Sensitivity to spatiotemporal color contrast in the peripheral visual field. *Vision Res.* **23**, 1–11.
- Nork, M. T., McCormick, S. A., Chao, G. -M. and Odom, V. (1990) Distribution of Carbonic Anhydrase Among Human Photoreceptors. *Inv. Ophthalm. Vis. Sci.* **31**(8), 1451–1458.
- O'Shea, R. P. and Williams, D. R. (1996) Binocular rivalry with isoluminant stimuli visible only via short-wavelength-sensitive cones. *Vision Res.* **36**(11), 1561–1571.
- Oyster, C. W. (1999) *The human eye: structure and function*. Sinauer Associates, Inc.
- Padmos, P. and Norren, D. V. (1975) Cone systems interaction in single neurons of the lateral geniculate nucleus of the macaque. *Vision Res.* **15**, 617–619.
- Petry, H. M. and Hárosi, F. I. (1990) Visual pigments of the tree shrew (*tupaia belangeri*) greater galago (galago crassicaudatus): a microspectrophotometric investigation. *Vision Res.* **30**, 839–851.
- Peng, Y. -W., Blackstone, C. D., Haganir, R. L. and Yau, K. -W. (1995) Distribution of glutamate receptor subtypes in the vertebrate retina. *Neuroscience* **66**(2), 483–497.
- Pugh, Jr. E. N. and Larimer, J. (1980) Test of the identity of the site of blue/yellow hue cancellation and the site of chromatic antagonism in the  $\pi_1$  pathway. *Vision Res.* **20**, 779–788.
- Pugh, Jr. E. N. and Mollon, J. D. (1979) A Theory of the  $\pi_1$  and  $\pi_3$  color mechanisms of Stiles. *Vision Res.* **19**, 293–312.
- Qin, P. and Pourcho, R. G. (1995) Distribution of AMPA-selective glutamate receptor subunits in the cat retina. *Brain Res.* **710**, 303–307.
- Rodieck, R. W. (1998) *The First Steps in Seeing*. Sinauer Associates, Inc.
- Rodieck, R. W. (1991) Which cells code for color. In A. Valberg and B. Lee, *From pigments to perception* (pp. 83–93). Plenum Press, New York.
- Röhlich, P., Ahnelt, P. K., Dawson, W. W. and Szél, A. (1994) Presence of immunoreactive blue cones in the fetal monkey fovea. *Exp. Eye Res.* **58**, 249–252.
- Roorda, A. and Williams, D. R. (1999) The arrangement of the three cone classes in the living human eye. *Nature* **397**, 520–522.
- Seidemann, E., Poirson, A. B., Wandell, B. A. and Newsome, W. T. (1999) Color signals in area MT of the macaque monkey. *Neuron* **24**(911), 917.
- Sekiguchi, N., Williams, D. R. and Brainard, D. H. (1993) Efficiency in detection of isoluminant and isochromatic interference fringes. *J. Opt. Soc. Amer. A* **10**, 2118–2133.
- Shapiro, M. B., Schein, S. J. and de Monasterio, F. M. (1985) Regularity and structure of the spatial pattern of blue cones of macaque retina. *J. Amer. Statistical Assoc.* **80**(392), 803–814.
- Shiels, R. and Falk, G. (1995) Signal transduction in retinal bipolar cells. *Prog. Retinal Eye Res.* **14**, 223–247.
- Shinomori, K., Spillmann, L. and Werner, J. S. (1999) S-cone signals to temporal OFF-channels: asymmetrical connections to postreceptor chromatic mechanisms. *Vision Res.* **39**, 39–49.
- Sperling, H. G., Johnson, C. and Harwerth, R. S. (1980) Differential spectral photic damage to primate cones. *Vision Res.* **20**, 1117–1125.
- Sterling, P. (1999) Deciphering the retina's wiring diagram. *Nature Neurosci.* **2**(10), 851–853.
- Stiles, W. S. (1949) Investigation of the Scotopic and Trichromatic Mechanisms of Vision by the Two-Color Threshold Technique. *Rev. d'Opt.* 139–163.
- Stiles, W. S. (1978) In *Mechanisms of color vision*. (ed. J. D. Mollon), Academic Press, London.
- Stockman, A., MacLeod, D. I. and Lebrun, S. J. (1993) Faster than the eye can see: blue cones respond to rapid flicker. *J. Opt. Soc. Am. A* **10**(6), 1396–1402.
- Stromeyer, C. F., Kranda, K. and Sternheim, C. E. (1978) Selective chromatic adaptation at different spatial frequencies. *Vision Res.* **18**, 427–438.
- Szél, A., Diamantstein, T. and Röhlich, P. (1988) Identification of the blue-sensitive cones in the mammalian retina by anti-visual pigment antibody. *J. Comp. Neurol.* **273**, 593–602.
- Szél, A., Csorba, G., Caffé, A. R., Szél, G., Röhlich, P. and van Veen, T. (1994) Different patterns of retinal cone topography in two genera of rodents, Mus and Apodemus. *Cell Tissue Res.* **276**, 143–150.
- Szél, A., Röhlich, P., Caffé, A. R. and van Veen, T. (1996) Distribution of photoreceptors in the mammalian retina. *Microsc. Res. Tech.* **35**, 445–462.
- Tovee, M. J. (1994) The molecular genetics and evolution of primate color vision. *Trends in Neurosci.* **17**(1), 30–37.
- Tovee, M. J., Bowmaker, J. K. and Mollon, J. D. (1992) The relationship between cone pigments and behavioural sensitivity in a New World monkey (*Callithrix jacchus jacchus*). *Vision Res.* **32**, 867–878.
- Troilo, D., Howland, H. C. and Judge, S. J. (1993) Visual optics and retinal cone topography in the common marmoset (*callithrix jacchus*). *Vision Res.* **33**(10), 1301–1310.
- Valberg, A., Lee, B. B. and Tigwell, D. A. (1986) Neurons with strong inhibitory S-cone inputs in the macaque lateral geniculate nucleus. *Vision Res.* **26**, 1061–1064.
- Vardi, N., Matesic, D. F., Manning, D. R., Liebman, P. A. and Sterling, P. (1993) Identification of a G-protein in depolarizing rod bipolar cells. *Visual Neurosci.* **10**, 473–478.
- Vardi, N., Morigiwa, K., Wang, T. -L., Shi, Y. -Y. and Sterling, P. (1998) Neurochemistry of the mammalian cone 'synaptic complex'. *Vision Res.* **38**, 1359–1369.
- Vardi, N., Duvoisin, R., Wu, G. and Sterling, P. (2000) Localization of mGluR6 to dendrites of ON bipolar cells in primate retina. *J. Comp. Neurol.* **423**, 402–412.

- Wandell, B. A. (1995) *Foundations of vision*. Sinauer Associates, Inc.
- Wandell, B. A., Poirson, A. B., Newsome, W. T., Baseler, H. A., Boynton, G. M., Huk, A., Gandhi, S. and Sharpe, L. T. (1999) Color signals in human motion-selective cortex. *Neuron* **24**, 901–909.
- Wässle, H. and Boycott, B. B. (1991) Functional architecture of the mammalian retina. *Physiol. Rev.* **71**, 447–480.
- Wässle, H., Grünert, U., Martin, P. R. and Boycott, B. B. (1994) Immunocytochemical characterization and spatial distribution of midget bipolar cells in the macaque monkey retina. *Vision Res.* **34**, 561–579.
- Weinrich, M. and Zrenner, E. (1983) Color-opponent mechanisms in cat retinal ganglion cells. In *Color Vision: Physiology and Psychophysics* (eds. J. Mollon and L. Sharpe), pp. 183–194. Academic Press, New York, NY.
- Wiesel, T. N. and Hubel, D. H. (1966) Spatial and chromatic interactions in the lateral geniculate body of the rhesus monkey. *J. Neurophysiol.* **29**, 1115–1156.
- Wikler, K. C. and Rakic, P. (1990) Distribution of photoreceptor subtypes in the retina of diurnal and nocturnal primates. *J. Neurosci.* **10**(10), 3390–3401.
- Williams, D. R. (1986) Seeing through the photoreceptor mosaic. *Trends in Neurosci.* **9**, 193–198.
- Williams, D. R. and Coletta, N. J. (1987) Cone spacing and the visual resolution limit. *J. Opt. Soc. Am. A* **4**, 1514–1523.
- Williams, D. R., Collier, R. J. and Thompson, B. J. (1983) Spatial resolution of the short wavelength mechanism. In *Color vision: physiology and psychophysics* (eds. J. Mollon and L. Sharpe), pp. 487–503. Academic Press, New York, NY.
- Williams, D. R., MacLeod, D. I. A. and Hayhoe, M. M. (1981a) Foveal tritanopia. *Vision Res.* **21**, 1341–1356.
- Williams, D. R., MacLeod, D. I. A. and Hayhoe, M. M. (1981b) Punctate sensitivity of the blue-sensitive mechanism. *Vision Res.* **21**, 1357–1375.
- Williams, D., Sekiguchi, N. and Brainard, D. (1993) Color, contrast sensitivity, and the cone mosaic. *Proc. Nat. Acad. Sci. USA* **90**, 9770–9777.
- Williams, D. R., Sekiguchi, N., Haake, W., Brainard, D. and Packer, O. (1991) The cost of trichromacy for spatial vision. In *From pigments to perception* (eds. A. Valberg and B. B. Lee), pp. 11–22. Plenum Press, New York.
- Willmer, E. N. and Wright, W. D. (1945) Color sensitivity of the fovea centralis. *Nature* **156**, 119.
- Wisowaty, J. J. and Boynton, R. M. (1980) Temporal modulation sensitivity of the blue mechanism: measurements made without chromatic adaptation. *Vision Res.* **20**, 895–909.
- Wysocki, G. and Stiles, W. S. (1983) *Color science: concepts and methods, quantitative data and formulae*. 2nd Edn. Wiley, New York, NY.
- Zhou, Z. J., Marshak, D. W. and Fain, G. L. (1994) Amino acid receptors of midget and parasol ganglion cells in primate retina. *Proc. Nat. Acad. Sci. USA* **91**, 4907–4911.
- Zrenner, E. (1983a) Neurophysiological aspects of color vision in primates. Comparative studies on simian retinal ganglion cells and the human visual system. Monograph. *Studies of Brain Function* Vol. **9** (eds. V. Braitenberg, H. B. Barlow, T. H. Bullock, E. Florey, O. -J. Grüsser, A. Peters), Springer, Berlin.
- Zrenner, E. (1983b) Neurophysiological aspects of color vision mechanisms in the primate retina. In *Color vision: physiology and psychophysics* (eds. J. Mollon and L. Sharpe), pp. 211–223. Academic Press, New York, NY.
- Zrenner, E. and Gouras, P. (1981) Characteristics of the blue sensitive cone mechanism in primate retinal ganglion cells. *Vision Res.* **21**, 1605–1609.